MiniBooNE Technical Note 74: Tests of the Scintillation Properties of Mineral Oil at IUCF

Patrick Ockerse, Sara Breitzmann, Chris Cox, Teppei Katori,
Shawn McKenney, Hans-Otto Meyer, Jen Raaf, Rex Tayloe, Nate Walbridge

February 5, 2003
Revised: April 26, 2003

Abstract

Experimental tests of the scintillation properties of mineral oil have been conducted at the Indiana University Cyclotron Facility. The measured scintillation light output of the MiniBooNE detector mineral oil, Marcol 7, from 180 MeV protons is $4.7 \pm 0.1 \pm 0.7$ photoelectrons/MeV corrected to 100% detected solid angle. The time distribution of this light is well-fit to a single exponential distribution with a characteristic time of 18.6 ± 1.0 ns. In addition, other tests were performed on a variety of oil samples with different additives.

1 Introduction

The MiniBooNE experiment at Fermilab uses a large mass ($\approx$ 800 tons) of mineral oil as a neutrino detector medium. It is important to understand the light production response to charged particles in this volume of oil. Čerenkov production is well-understood and depends only upon the density and index of refraction of the medium. Scintillation, however, depends on the details of the mineral oil composition and minute levels of contaminants and is not easily calculated. The scintillation light produced in mineral oil has been investigated at the Indiana University Cyclotron Facility (IUCF). The results from these investigations are reported here.

A method has been developed and implemented at IUCF to measure the amount and time distribution of scintillation light produced by 180 MeV (kinetic energy) protons as they traverse a small sample of mineral oil. The amount of light seen in this tests is quite small — typically only several photoelectrons are observed in each event. The number of photoelectrons can be measured (Section 3.1) and, therefore, these low-light level tests allow for an absolute measurement to be made without the need for a calibrated light source. These protons are below the threshold for Čerenkov light production ($T_{\mathrm{threshold}} = 341$ MeV) so the light observed is, to a high degree of certainty, exclusively from scintillation in the mineral oil (Section 3.3.4).

Tests have been performed during the last two years. The latest tests concentrated on measuring the properties of the mineral oil selected for MiniBooNE, Marcol 7. Measurements of this oil were made to extract the absolute scintillation output and time distribution of the produced light. Also investigated were samples of Marcol 7 with different scintillator additives as well as samples of Marcol 7 saturated with nitrogen, oxygen, BHT, and Vitamin E. In addition, several measurements were made to check the reproducibility of the tests and the interpretation of the results.

2 Experiment

In 2002, three separate test sessions were conducted using the 205 MeV IUCF proton beam. These were in January (01/02), March (03/02), and July (07/02). In 2001, there was one test session in March (03/01).

Oil (short name)	Oil (full name)	Manufacturer	density (g/cm^3)
M7	Marcol 7	Exxon/Mobil	0.845
Witco	Witco scintillator fluid	Witco (now Crompton)	0.837
Drakeol	Penreco Drakeol 5	Penreco/Pennzoil	0.831
Amaco	Amaco Superla 5	Amaco (now Chevron)	0.834
Ispoar L	Isopar L parafinnic solvent	Exxon	0.760
Ispoar M	Isopar M parafinnic solvent	Exxon	0.784

Table 1: Summary of pure mineral oils tested. The Marcol 7 samples were obtained from 12/01 through 6/02. The other samples were transfered to IUCF in 2/01. With the exception of the Witco sample, they were procured for tests at FNAL in mid-late 2000. The Witco sample had been procured somewhat earlier. The densities were measured at IUCF and have a 0.001 g/cm^3 error.

Sample #	Location of oil	Date poured
S1	first railcar	12/19/01
S2	first railcar (different beaker)	12/19/01
S3	overflow tank	12/19/01
S4	tank bottom	5/14/02
S5	overflow tank fill line	6/01/02
S6	fill line after 175 kgallon recirculation	6/26/02

Table 2: Summary of Marcol 7 oil samples along with the location and date that each sample was poured. Sample #6 best represents the oil that is currently in the MiniBooNE tank.

2.1 Samples Tested

A total of six different mineral oils have been tested at IUCF. In 2001, five different candidate mineral oils for MiniBooNE were tested. The 2002 tests concentrated on measurements of the mineral oil selected for miniBooNE, Marcol 7 (M7). Marcol 7 is manufactured by Exxon/Mobil and originates in Houston, Texas. These six oils are summarized in Table 1.

Six samples were drawn at FNAL from the Marcol 7 oil used in MiniBooNE. These six samples are summarized in Table 2. The standard sample #1 was poured from the first rail car and was tested several times to check reproducibility. Another sample (#2) was poured from the same rail car and was tested to check that the results did not depend on the details of the specific sample container. A sample (#3) was poured from the MiniBooNE overflow tank during the filling of the main tank and was tested to see if any effect of residual scintillator could be seen. Sample #4 came from the bottom of the main tank about one month after the main tank was filled completely. Sample #5 was poured from the overflow tank fill line about two months after the main tank was filled completely. Sample #6 was poured from the fill line after recirculating 175,000 gallons of oil in the main tank and, of the samples tested, best represents the oil that is currently in the MiniBooNE tank. These samples were transported to IUCF in plastic containers and then transfered to glass. Tests show that that there is no difference between oil stored in plastic for a short time and oil stored in glass. However, the samples were transferred to glass for long-term storage.

To test the response of M7 to scintillator, the standard M7 was mixed with two types of scintillator, Butyl PBD (PBD) and Methylcarbozole (MC), at a concentration of 0.01 g/l. In the 2001 tests, PBD and MC in dilute concentrations (0.01–2.0 g/l) were tested with Witco and Isopar L. To test the effects of common antioxidant additives to mineral oil, the standard M7 was mixed with 1 g/l of Vitamin E and with 1 g/l of BHT (Butylated hydroxytoluene). To get a rough idea of the effects of bubbling gases through mineral oil, two samples were prepared by vigorously bubbling one with oxygen (O_2) and and one with nitrogen (N_2) for several days. It was assumed, that these samples were saturated with these gases.

In addition, to study systematic uncertainties, an empty sample container, a sample of deionized water, and two different thin scintillator sheets of 1mm thickness were tested.

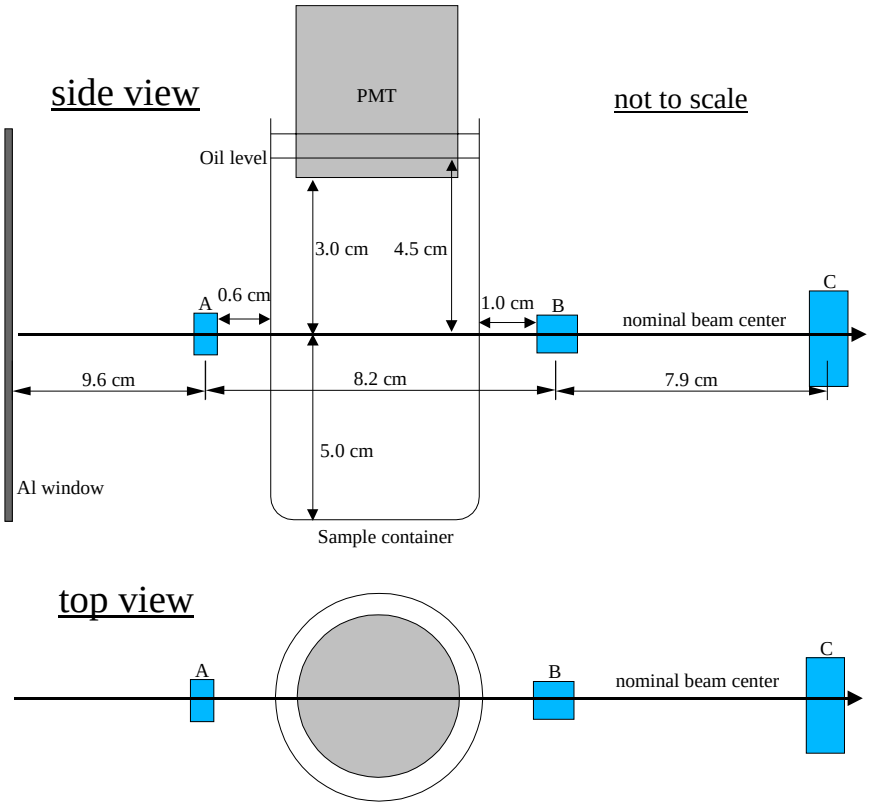

Figure 1: A schematic of the detector setup for the oil tests. A, B, and C are the trigger scintillators. This apparatus is enclosed in a light-tight box. For the 2002 runs, the apparatus had to be rotated by 180 degrees such that the beam direction was reversed from that shown (because of space constraints in the RERP area).

2.2 Proton Beam

The tests were performed using the IUCF proton beam in the Radiation Effects Research Program (RERP) test area. The IUCF main-stage cyclotron delivered 205 MeV protons at a rate of approximately 10KHz, controlled and monitored by the cyclotron operators for these tests. The proton rate varied from 1-50 kHz during the duration of the tests. The beam was spread to approximately 10cm in diameter at the location of the oil sample by an upstream copper spreader (0.24 cm thick). By spreading the beam in this way, the proton tracks through the sample was the same throughout the tests, and did not depend on the details of beam focusing.

In the 2001 tests, the RERP area was located about 25 meters from the main-stage cyclotron. Before the 2002 tests, the beamline was reconfigured and lengthened such that test area was moved to approximately 50 meters from cyclotron. In addition, the beam line terminated much closer to a shielding wall that necessitated a 180 degree rotation of the test apparatus. A degrader system, consisting of a movable ladder with differing thicknesses of copper plates, was employed for a several tests in 2001. This can be used to "degrade" the beam energy to study saturation in the oil samples. It was not used in 2002.

2.3 Apparatus

The apparatus used for these tests is shown schematically in Figure 1. It consisted of three trigger scintillators (NE102) (A, B, and C) viewed by RCA8575-equivalent photomultiplier tubes (PMTs) aligned on the nominal beam center. A fourth scintillator (Z), viewed by an RCA8575-equivalent PMT was placed upstream of the apparatus in the earlier tests to monitor the beam rate. It was determined to be superfluous and not used in the later tests. The sample container was placed in between scintillators A and B and was viewed with a Burle 8850 51mm diameter 12-stage Pyrex-window Quantacon PMT (S) [1]. This tube was run at 2800-

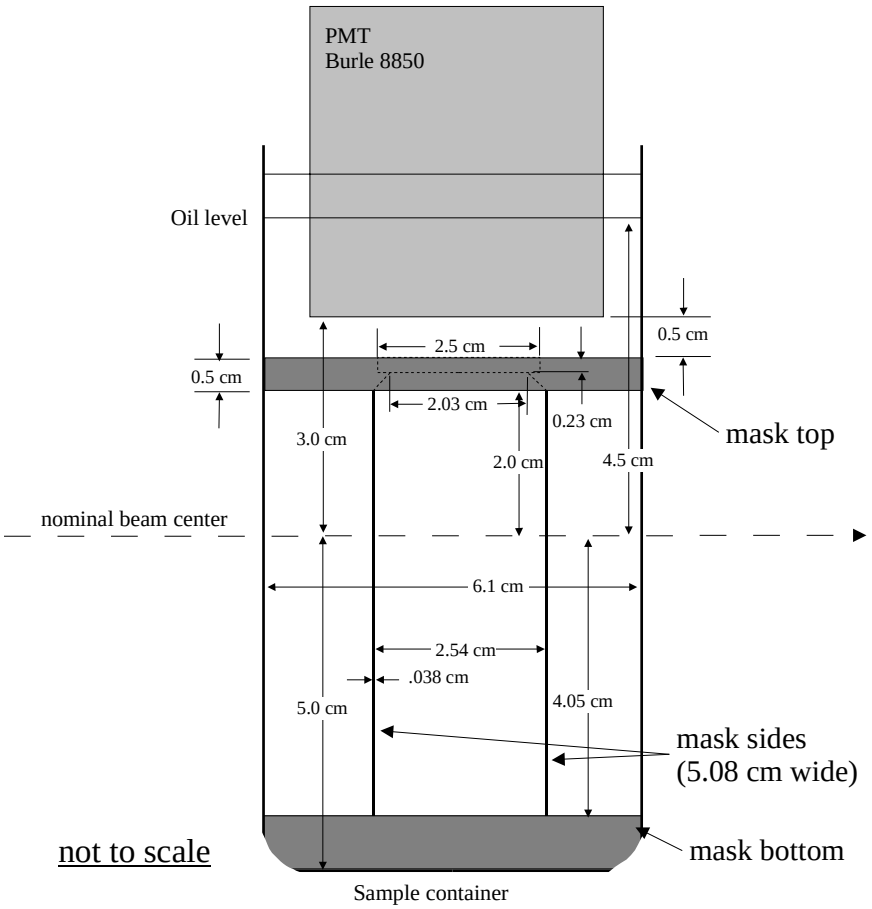

Figure 2: A schematic drawing of the sample container with mask system used for the oil tests.

2900 Volts and used a base that provided 33% of this voltage across the photocathode and first dynode as recommended by the manufacturer. This was crucial to achieve the single-photoelectron resolution necessary to measure these low-light levels. The sample PMT and base were mounted on a movable rail system so that it would be easily lifted to change the oil sample. During the testing, the PMT was partially immersed into the oil such that the end window was 3.0 cm from the nominal beam center.

The sample containers were 300mL PYREX beakers lined on the sides and bottom with black-anodized 10mil aluminum sheets. The aluminum greatly reduced reflected light from reaching the sample PMT. Several dozen of these sample containers were used throughout the tests to allow all oil samples to be prepared ahead of time.

For the 2002 tests, a mask system, shown schematically in Figure 2 was fabricated to allow the use of "plugs" and filters. The plugs were anodized aluminum disks with holes of different sizes to reduce the solid angle viewed by the PMT. This system changed the effective solid angle viewed by the PMT from 7.3% (no mask system) to 4.0% (with the mask system). The addition of the plugs allowed the solid angle to be further reduced in 5 steps down to 0.1%. In addition, the mask system reduced the viewable proton path length in the oil sample from 6.1 cm to 2.5 cm. This system also held the neutral density and bandpass filters and had side walls to reduce the visible path length of the proton tracks in the mineral oil. This system was black-anodized and fit snuggly inside the sample container.

Also, for the 2002 tests, a magnetic shield was fabricated that fit over the PMT and sample container yet was not in the beam path defined by the three trigger scintillators. It was determined in separate tests that this effectively shielded the PMT from stray magnetic fields which can reduce the measured light by as much as a factor of 2 for a 2 Gauss field.

This apparatus was enclosed in a light-tight "darkbox". The darkbox had a side door which allowed for

quick access to change samples. For the proton beam tests, the darkbox was placed on a movable table and aligned to the nominal beam center.

The signals from the PMTs were routed on coaxial cables out of the RERP area and into amplifiers. The amplified signal was split, one path was routed to an ADC, the other was discriminated and routed to a TDC and used for the trigger. The trigger condition was a coincidence of the A, B, and C scintillators. A 130ns gate was formed and used for the ADC. This gate width was shortened to 60ns to combat a noise problem for some of the 2002 tests. Noise on the small signals from the sample PMT was an ongoing problem and was lessened with filters placed at various locations within the signal path. The digitized ADC and TDC signals histogrammed online and stored to disk for later analysis. The trigger rate was approximately 1kHz and a typical run consisted of 100-500k triggered events.

3 Analysis

The event data were analyzed after the beam tests to histogram the ADC and TDC values and to create an ntuple that could later be used to create selected time distributions.

3.1 Strength of Scintillation Light: ADC Analysis

Requiring a coincidence of the three trigger scintillators provides for a clean beam signal so no additional offline cuts were needed for the analysis of the sample tube ADC signals. The ADC values were used to fill several different histograms so that the optimal binning could be chosen, but the histograms created online would have been sufficient for this analysis.

The ADC distributions were fit to a Gaussian-convoluted Poisson distribution of the form:

$$\begin{aligned} f(X) &= \frac{1}{\sqrt{2\pi}}\frac{P_2}{P_4}\sum_{n=0}^{n_{\max}}\frac{1}{n!}P_1^n e^{-P_1}\frac{1}{\sqrt{\sigma_n}}e^{\frac{(X_{\mathrm{pe}}-n)^2}{(2\sigma_n^2)}}, \\ X_{\mathrm{pe}} &= (X-P_3)/P_4, \\ \sigma_n &= \begin{cases} P_5 & n=0 \\ P_6 n^{P_7} & n>0, \end{cases} \end{aligned}$$

where X is the ADC value and n is the number of photoelectrons ($n = 0$ corresponds to the pedestal). The P_i are the seven parameters that could be fit to a particular distribution. P_1 is the Poisson mean and referred to as "μ". This is the average number of photoelectrons detected by the PMT. P_2 is a normalization parameter. P_3 is the offset or ADC position of the pedestal. P_4 is the "gain" in ADC channels/photoelectron. P_5, P_6, and P_7 are parameterizations of the width of the Gaussian distribution. A plot of an ADC spectrum obtained in the lab with an LED light source showing the individual photoelectron peaks and the contributing Gaussian distributions is shown in Figure 3.

Of course, a seven-parameter fit was not performed for every distribution. In practice, some distributions were used to obtain one of the parameters and then this parameter would be kept fixed for subsequent fits. For example, the offset (pedestal) was determined from a set of low-light distributions, and then was fixed for fits to subsequent high-light distributions where the pedestal could not be seen. The gain was also determined from low-light distributions where the individual photoelectron (PE) peaks could be seen. The gain had to be fixed for the high-light level distributions as it is impossible to fit both the gain and μ simultaneously. The results for two different fits for runs 574 and 581 are shown in Figures 4 and 5. The resulting μ values from these fits were 1.9 and 8.3 PEs.

The statistical error on the resulting fit parameters was negligibly small — the dominant error was systematic and determined by comparing fits of different ranges and to different distributions. It was determined that for fits with μ greater than 1.0 the systematic error on $\delta\mu/\mu$ was 10%. For fits with μ less than 0.1 a 100% error was assigned due to the high-sensitivity of these fits to the particular value for the parameters chosen and due to the small contamination possible from Čerenkov light (discussed below). For fits with μ between 0.1 and 1.0, an error between 10% and 50% was assigned depending on the quality of the fit and the sensitivity to the fixed fit parameters.

It is important to remember that this analysis procedure, if carefully performed sets an absolute scale for number of photoelectrons observed and eliminates uncertainty in absolute light calibration. If the individual

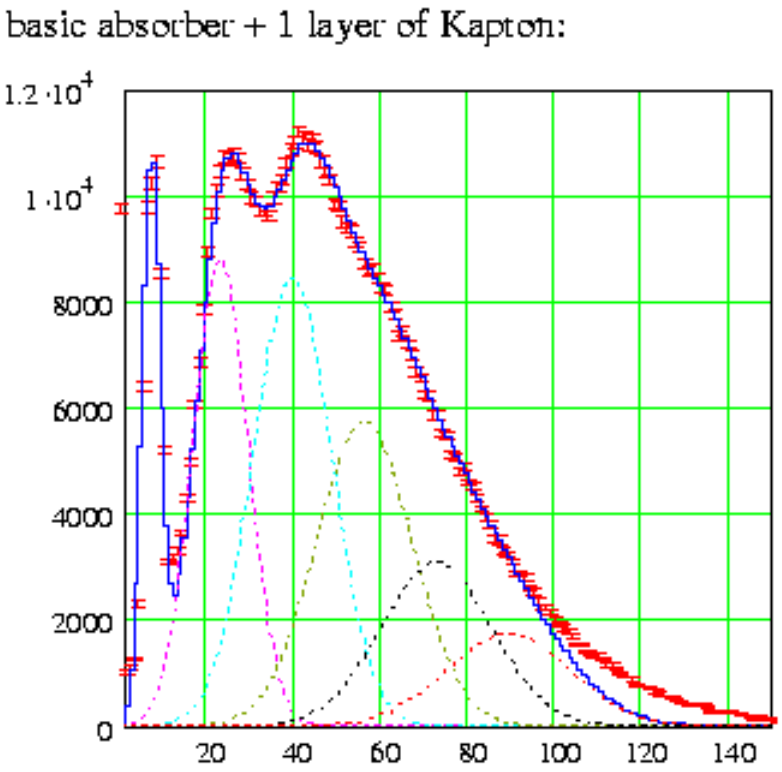

Figure 3: An ADC distribution obtained in the lab with an LED light source showing the locations of the individual photoelectron peaks. The sharp peak at the left is the ($n = 0$) pedestal.

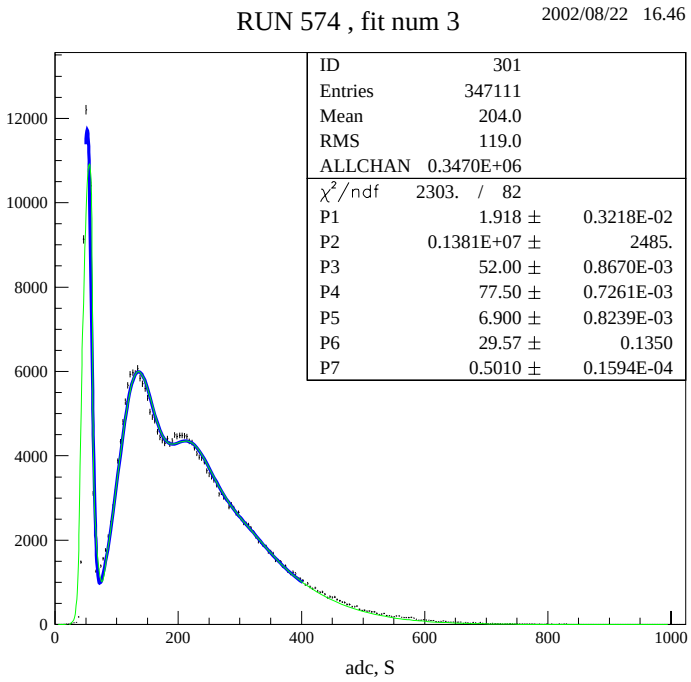

Figure 4: The ADC distribution for run 574. The pedestal (0 PE) as well as the the first and second PE peaks can be seen. The parameters obtained are shown in the inset ($\mu = 1.9$). The dark line indicates the value fit function in the range of the fit, the light line shows the function extrapolated outside of the range.

PE peaks are correctly fit in the low-light level runs and the gain and offset remains constant (within errors), then the PE scale is correctly set.

3.2 Time Distribution of Scintillation Light: TDC Analysis

To determine the time distribution of the light emitted in a particular mineral oil, dedicated runs were performed with the mask system in place to lower the light level observed. This is necessary because the TDC on the sample tube is stopped by the first observed photoelectron, and, if a particular sample emits multiple PEs, the time distribution will be distorted. In addition to using low-light level runs for this analysis, the data was analyzed off-line to select events where only one PE was emitted. This was accomplished by applying a cut to the ADC value that selected single-PE events. For these events, the time was calculated (20 TDC channels = 1 ns) and histogrammed. This procedure is illustrated in Figure 6.

The time distributions were then fit to an exponential distribution. It is expected that some oil samples will produce light with more than one characteristic time [2]. If a time distribution did not fit well to one exponential, two fits were performed on different time ranges.

3.3 Monte Carlo

A GEANT-based [3] program (`tstoil`) was written to simulate the IUCF miniBooNE oil-test setup. The geometry of the setup was coded into the program, protons were tracked through the setup, and various quantities were stored in a PAW ntuple. This information was then used to determine the energy of the protons at the sample, the energy loss of the protons within the sample, the effective solid angle subtended by the sample PMT, and the expected number of Čerenkov photons detected.

3.3.1 Geometry

The geometry of the oil test setup was coded into the `tstoil` program with all materials that were traversed by the proton beam described in detail. The program described 3 m of beam pipe (with vacuum), including

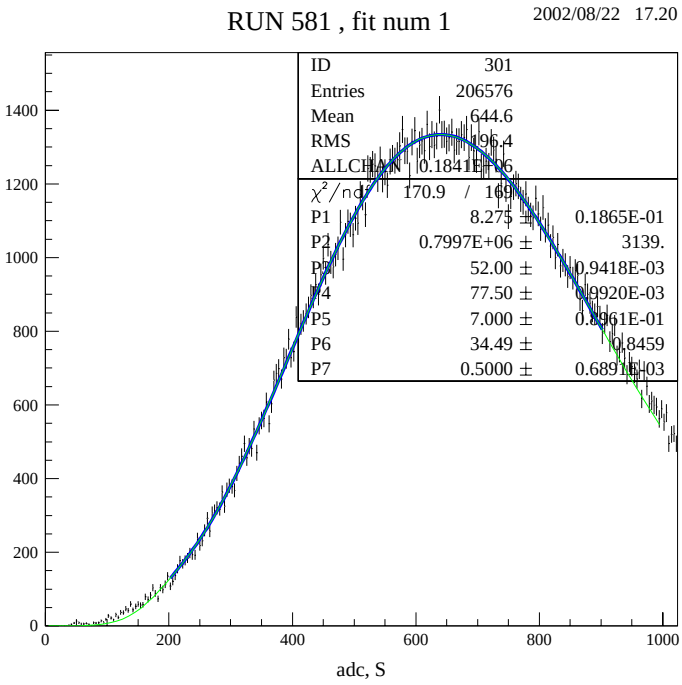

Figure 5: The ADC distribution for run 581. The parameters obtained are shown in the inset ($\mu = 8.3$). The dark line shows the value of the fit function in the range of the fit, the light line shows the function extrapolated outside of the range.

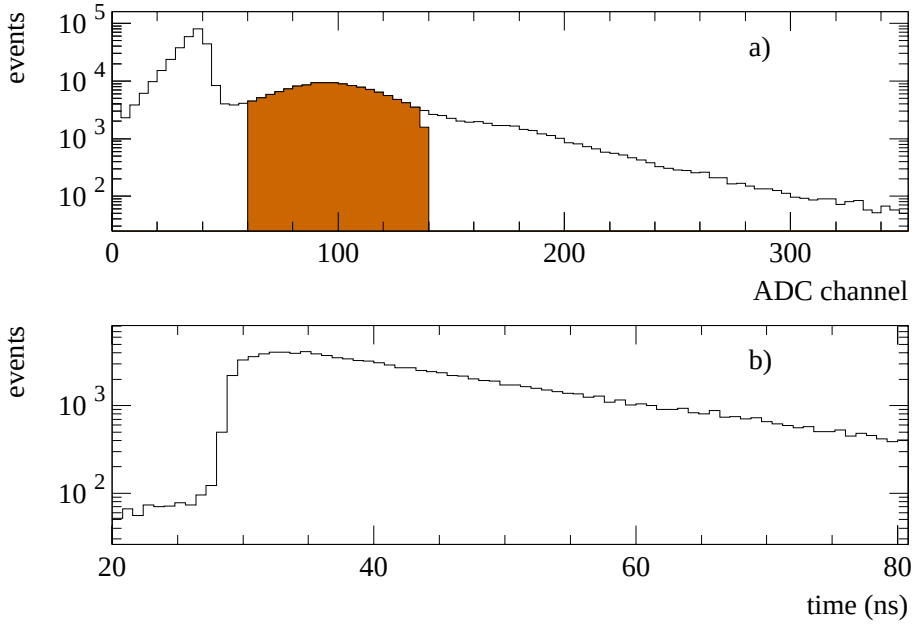

Figure 6: ADC (a) and time (b) distributions from Run 144 for pure M7 with a mask to reduce the effective solid angle and, therefore, the amount of light. The shaded area in (a) indicates the cut applied to produce the time distribution in (b).

object	z-pos (cm)	thickness (cm)	material
spreader	-320.7	0.24	Copper
sem foils	-107.	0.02	Copper
mylar window	-59.1	0.01	Carbon (mylar)
degrader	-42.	varying	Copper
scint Z	-29.6	0.64	Scintillator
box window	-13.4	0.022	Aluminum
sample beaker	0.0	see text	various
scint A	-3.83	0.64	Scintillator
scint B	4.23	1.27	Scintillator
scint C	12.13	1.27	Scintillator

Table 3: Center position, thickness, and material for the beamline components important for energy loss.

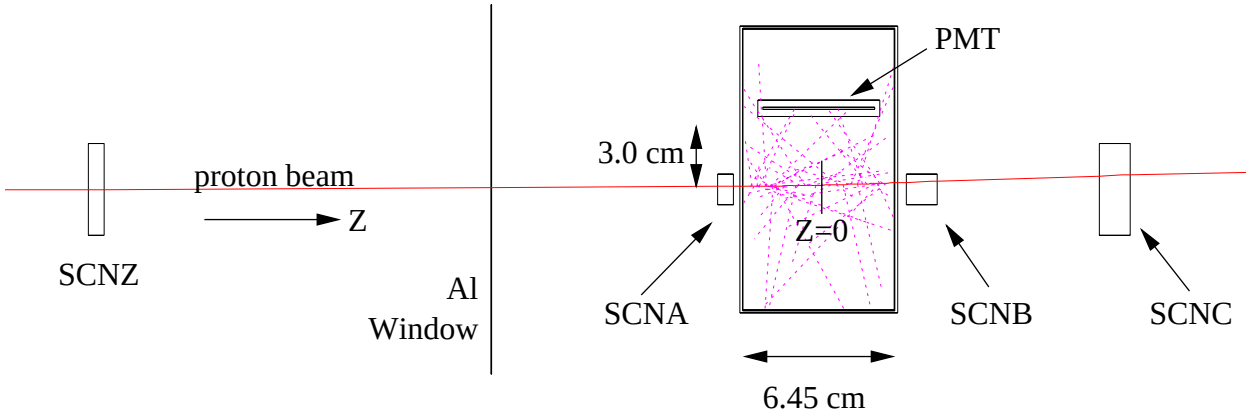

Figure 7: Schematic drawing (side view) of the simulation setup as coded into the simulation program. The tracks of the incident proton beam and generated photons in the oil sample are shown.

the Cu spreader, SEM foils, collimator, and mylar window. Downstream of the beampipe, the volumes described were the degrader, scintillator-Z, test-box window, scintillator-A, sample beaker, scintillator-B, and scintillator-C. The position and thickness of these items are given in Table 3 and shown in Figure 7. The sample beaker was modeled as a cylinder of glass (SiO_2), of outside diameter 6.45 cm and thickness 0.1 cm with a 0.025 cm lining of black aluminum inside. The mineral oil volume was modeled as a cylinder inside of the beaker with diameter 6.2 cm. A nominal density of 0.845 gm/cm^3 was used to simulate the M7 mineral oil, the energy loss was scaled to account for the different density of the other mineral oils tested.

A model for the PMT was coded into the program. This model consisted of a glass disk with an thin layer of Aluminum embedded inside. The glass disk of diameter 50 mm simulates the glass envelope of the tube. The thin Al layer of diameter 46 mm models the photocathode of the tube. The details of these simulated volumes were changed in the program to reflect the changes in the experimental setup in the different test periods.

3.3.2 Tracking

The simulation started the proton at $z = -330$ with kinetic energy of 205 MeV and direction along the z-axis. The proton was then tracked through the various materials described in the setup with full accounting of the energy loss, multiple scattering, and hadronic interactions. By starting the proton at this location, upstream of the spreader, and modeling the multiple scattering, an accurate representation of the beam position and divergence at the sample location was obtained.

As the proton was tracked through the mineral oil sample, production of both scintillation and Čerenkov

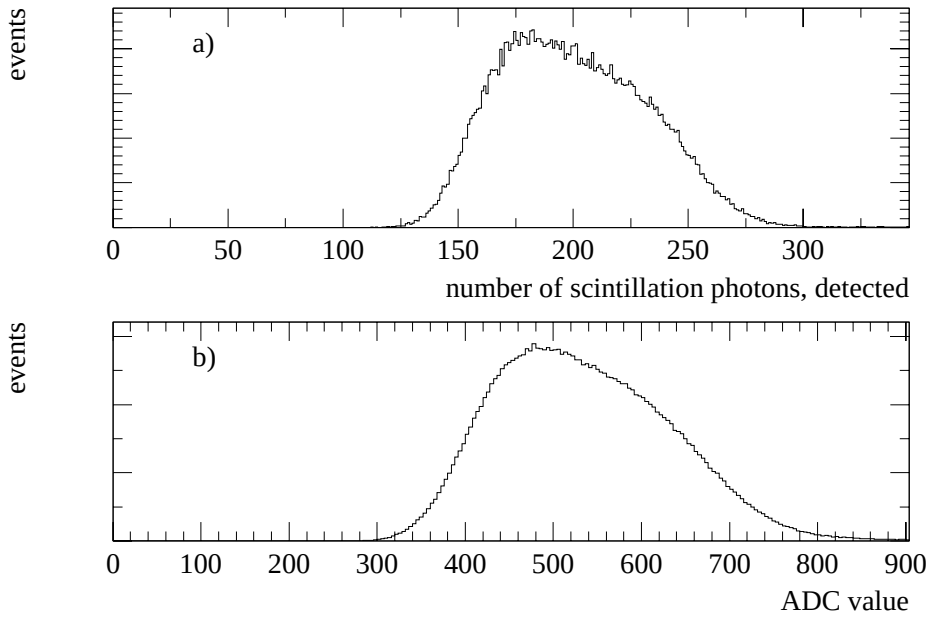

Figure 8: Distribution of the number of scintillation photons detected in the simulation for a large number generated (a) compared with the measured ADC spectrum for a high-light level run (b). The asymmetric shape of the ADC spectrum due to the integral over proton paths through the sample is well-reproduced by the simulation.

photons was simulated. The Čerenkov simulation of the GEANT package was used to model the production of Čerenkov photons in the oil sample. The primary proton is below threshold ($T_{\text{threshold}} = 341$ MeV) and does not directly produce Čerenkov light. However, the proton may produce delta-ray electrons above Čerenkov threshold, which will produce Čerenkov light (Section 3.3.4).

Scintillation photons were generated isotropically at each step of a charged particle. Since the number of photons generated in mineral oil was not known (that was the subject of the tests), 100 photons were generated for every 1 MeV of energy lost in the sample.

Both scintillation and Čerenkov photons were then tracked in the mineral oil sample. The optical properties of the mineral oil, black aluminum lining, and the PMT glass were all modeled. The mineral oil was modeled with an index of refraction of 1.47 and a large attenuation length (1000 m). The black aluminum lining was modeled with as a diffuse partial reflector with a 3% reflection probability. The PMT glass has the same optical parameters as the mineral oil. A photon was considered as detected if it hit the photocathode layer of the model PMT.

The detailed photon tracking allowed for an accurate estimate of the effective solid angle of the tube by counting the number of scintillation photons "detected" by the PMT and normalizing by the number produced. This technique produced a numerical integral of the effective solid angle of the PMT. The integral accounts for all possible photon paths from all possible points of origin on the proton track. The integral over all possible proton paths through the sample results in an asymmetric distribution of detected photons when the number of generated photons is large compared to Poisson fluctuations. This is reproduced accurately in the simulation as can be seen in Figure 8.

The production and tracking of the Čerenkov photons allows for an estimate of possible contamination by Čerenkov light in the predominantly scintillation signal.

Since all important materials in the proton path were modeled, the beam spread (and presumably, divergence) at the sample as predicted by the simulation should be accurate. The transverse location of the beam from the simulation is shown as a scatter plot in Figure 9. This agrees well with the transverse distribution of protons in the RERP area measured with an X-ray film exposed in the beam.

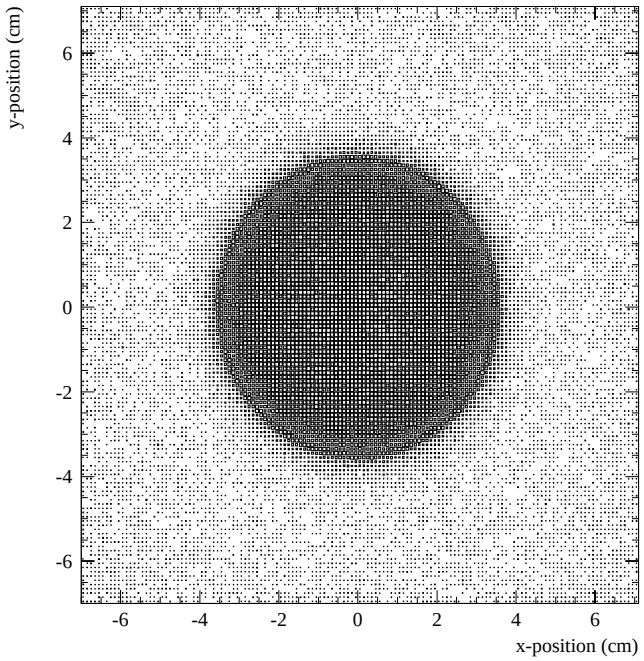

Figure 9: Box plot of the beam x and y approximately 13 cm upstream from the oil sample location as calculated by the simulation program.

Proton KE at sample	180 MeV
Energy loss within sample	28.0 MeV
Average Number of scintillation photons produced	2821
Average Number of scintillation photons detected	205.9
Effective PMT solid angle	7.30 %
Average Number of Čerenkov photons produced	13.7
Average Number of Čerenkov photons detected	0.59

Table 4: Typical results from simulation of the oil test setup.

3.3.3 Simulation Event Sample

To obtain an event sample from the simulation to use for data, cuts were applied to the raw sample to model the effect of the trigger scintillators. The energy loss for each of the trigger scintillators was recorded in the simulation and are shown in Figure10. The cut values were 2 MeV for the thinner A,Z scintillators and 4 MeV for the thicker B, C scintillators. The events that passed these cuts form a sample that is a good representation of the actual test data sample. The number of simulated protons that pass though all 4 trigger scintillators is about 0.8% of the generated sample.

3.3.4 Simulation Results

The results for the various quantities produced were tabulated and used for the calculation of results reported below. These results changed depending of the details of the test setup which changed from test to test. Typical values calculated are reported in Table 4.

The distributions of the number of produced and detected Čerenkov photons are shown in Fig. 11. These distributions show that the PMT efficiency in collecting Čerenkov light is affected by the directional nature of this light. It is important to remember when looking at the distribution of predicted number of detected Čerenkov photons that the PMT in the simulation is 100% efficient. To predict the actual number of detected

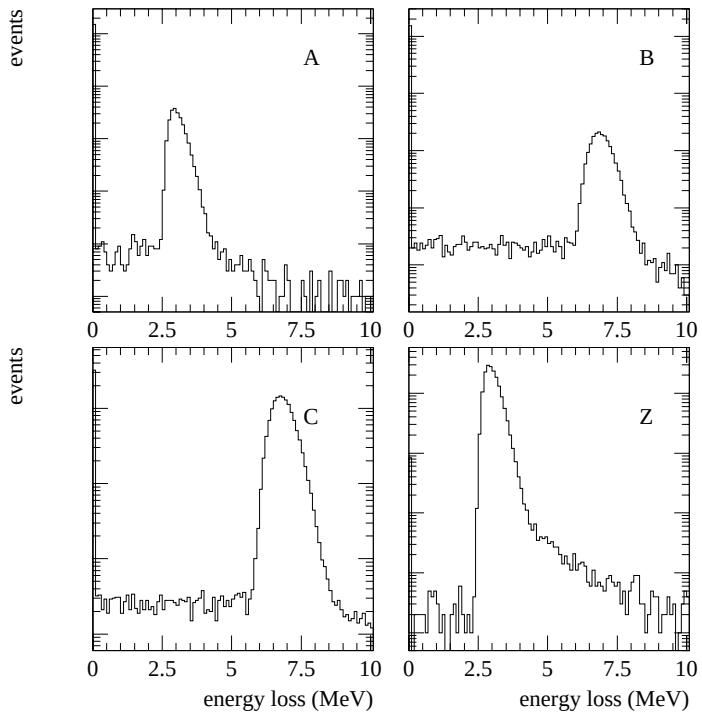

Figure 10: Distribution of simulated energy loss values in each of the 4 trigger scintillators.

Čerenkov photons, the quantum efficiency ($\approx 20\%$) of the PMT must be considered. When this is properly considered, the level of contamination from Čerenkov light is estimated to be less than 0.1 photoelectron. This is negligible compared to other sources of systematic error for high-light level tests and sets an upper limit on the tests that result in very low light levels.

The results produced by the simulation program for energy loss and Čerenkov production were checked for one of the configurations by hand calculation. The simulation and calculations were in agreement.

A relative error of 2.5% was assigned to the value calcuated for the proton energy loss in the mineral oil sample due to uncertainties in material thicknesses and densities. The error on the calculated solid angle subtended by the PMT was estimated to be 15% for the runs without the mask system and 10% for the runs with. These errors are due to the uncertainty in the PMT-proton track distance and the uncertainty in the effective PMT photocathode diameter. For the runs with the mask system, this is less uncertain as the better-known mask diameter determines this diameter.

3.4 Strength of Scintillation Light: δ

The amount of scintillation light is determined by the fits to the ADC distributions (Section 3.1) that result in a average number of photoelectrons (PEs) detected. In order to report a value that folds out the effects of PMT solid angle and proton energy loss, and new value, δ is formed. This value is defined

$$\delta = \frac{\mu}{\Delta E \, \frac{\Omega}{4\pi}}$$

where μ is the number of PEs as determined from the ADC fit, ΔE is the proton energy loss and $\frac{\Omega}{4\pi}$ is the solid angle fraction subtended by the PMT. The quantities ΔE and $\frac{\Omega}{4\pi}$ are determined from the simulation as described above. The units of δ are PE/MeV. The finite quantum efficiency of the PMT is not included in these calculations and should be kept in mind when drawing conclusions about the absolute number of *photons* produced.

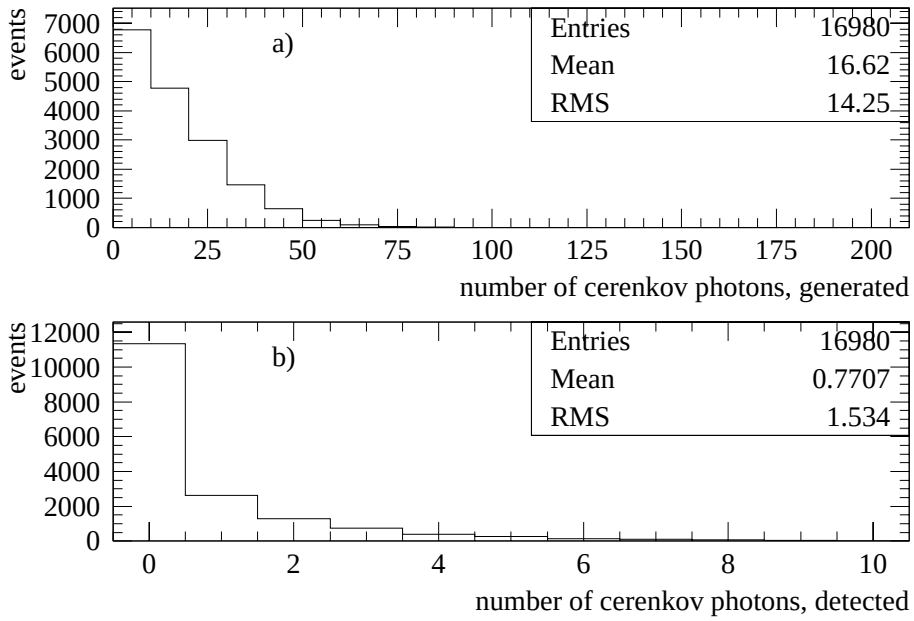

Figure 11: Distribution of the number of Čerenkov photons generated (a) and detected (b).

The errors contributing to the uncertainty in δ are due to the uncertainties, described above, in the three quantities : μ, ΔE, and $\frac{\Omega}{4\pi}$. They are typically 10%, 2.5%, and 15%, respectively. When added in quadrature a relative error on δ of 18% results. However, as the error in μ is most-likely uncorrelated between different fit values, it can be treated as a statistical error and will be reduced by a factor $1/\sqrt{N}$ in an average. The errors on ΔE and $\frac{\Omega}{4\pi}$ are assumed to behave as systematic errors and are correlated between tests. For this reason, they enter as an error on the δ scale in the final results.

A number of the tests in 07/02 were performed with the ADC gate width set to 60 ns. This caused a reduction in detected light due to the extended time distribution of the light output from Marcol 7. The characteristic time of this distribution was measured and used to correct the measured δ values by 7%.

4 Results

In the following section, results on the tests of mineral oil scintillation are reported. Emphasis is given to the results on mineral oil selected for the MiniBooNE experiment, Marcol 7 (M7). Many other tests, performed on other mineral oils with various additives and with slightly different configurations, are also reported.

4.1 Pure Marcol 7: Scintillation Light Strength

The measured δ values for various runs on pure M7, some from different samples, some with slightly different setups are plotted in Figure 12. The nominal configuration for these runs was with the PMT HV at 2900V and no attenuation of the signal.

As can be seen in Figure 12, the measured δ values from these runs are consistent within errors. There is a slight indication that the later runs are low compared to earlier. This is consistent with a systematic shift due to setup change, a chemical change of the oil over time, or an degradation of the PMT photocathode over time. However, these changes are slight and are not outside of the estimated systematic error.

The average δ for pure Marcol 7 from these runs is $4.7 \pm 0.1 \pm 0.7$ PE/MeV corrected to 100% solid angle. The first error is the systematic error in the μ fit (assumed uncorrelated). The second error is that due to the uncertainty in solid angle and energy loss.

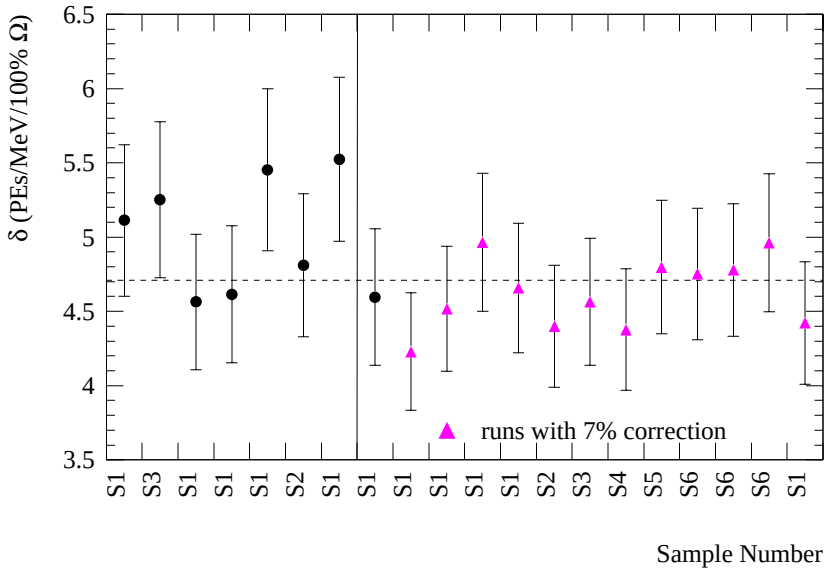

Figure 12: Measured δ values for pure Marcol 7 for 20 separate tests performed in 2002. The horizontal dotted line indicates the average value of 4.7 PE/MeV corrected for 100% solid angle. The error bars are due to the systematic error in the ADC fit. There a 15% error on the scale due to uncertainty in the PMT solid angle and the energy loss of the proton in the oil sample. All of the runs to the right of the solid vertical line were done in 07/02. The sample numbers are described in Table 2. The tests that were subject to a 7% correction due to a narrow ADC gate are indicated.

4.2 Pure Marcol 7: Scintillation Light Time Distribution

Using the procedure described in Section 3.2, the time distribution for pure Marcol 7 was extracted from low-light level runs (using the mask system). The distribution for a particular run is shown in Figure 13 together with the fit. An average value for all low-light pure M7 runs was 18.6 ± 1.0 ns. The error is quoted is purely systematic (the statistical error is negligible) and is due to the uncertainty on the fits and was estimated from the spread in the lifetimes obtained from the different samples, fit ranges, and the ADC cuts applied to obtain the time distributions. There is no evidence in this data on pure Marcol 7 for more than one time constant in the scintillation light.

4.3 Marcol 7 with Additives

The measured δ values for Marcol 7 samples with various additives for a set of runs taken in 01/02 are summarized in Table 5 and are plotted in Figure 14. The addition of 0.01 g/l PBD or MC increases the light output by about a factor of four. This was approximately the same relative change that was seen for the addition of this amount of PBD to Witco mineral oil in previous runs. It is somewhat surprising that the addition of MC increases the amount of light by the same factor as the PBD as it seemed to have a much smaller effect in previous runs. However, this was with a different mineral oil and at different concentrations so a direct comparison is not possible. And, as has been seen in these tests and is known, the light output with different concentrations of scintillator depends strongly on the solvent and does not change linearly with concentration [2].

The addition of 1 g/l of Vitamin E or BHT seems to *decrease* the scintillation light by a factor of 2.5. The sample of mineral oil saturated with oxygen has a light output reduced by a factor of 2.5. This effect on liquid scintillators is known [2]. It is interesting to verify it for pure mineral oil. The sample of mineral oil saturated with nitrogen, on the other hand, shows a slight increase in light output, presumably because the oxygen, which is known to decrease the light output, has been "flushed-out" by the nitrogen (Section 4.4).

Time distributions were obtained for samples of Marcol 7 with Scintillator additives. The time distributions and fits are shown in Figure 14 for M7+0.01 g/l PBD and M7+0.01 g/l MC together with those

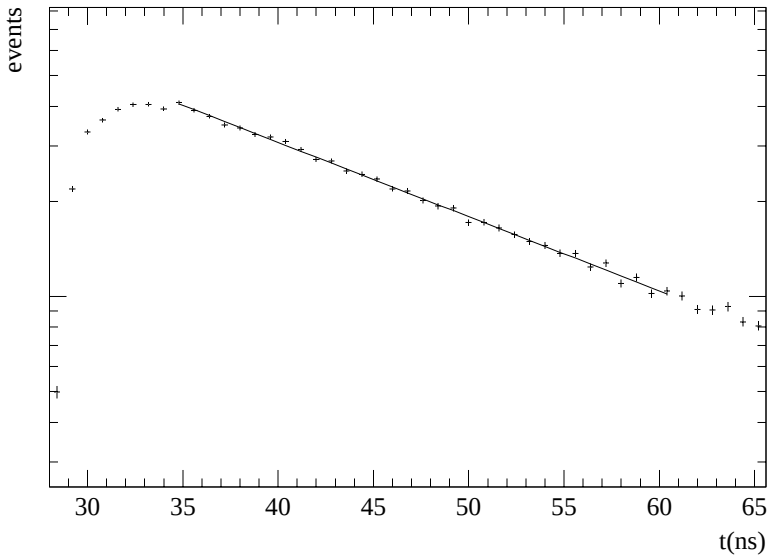

Figure 13: Time distribution and fit for pure Marcol 7, Run 144. The lifetime and statistical error deduced from this particular run and fit was $\tau = 18.5 \pm 0.1$ ns. Note the logarithmic scale.

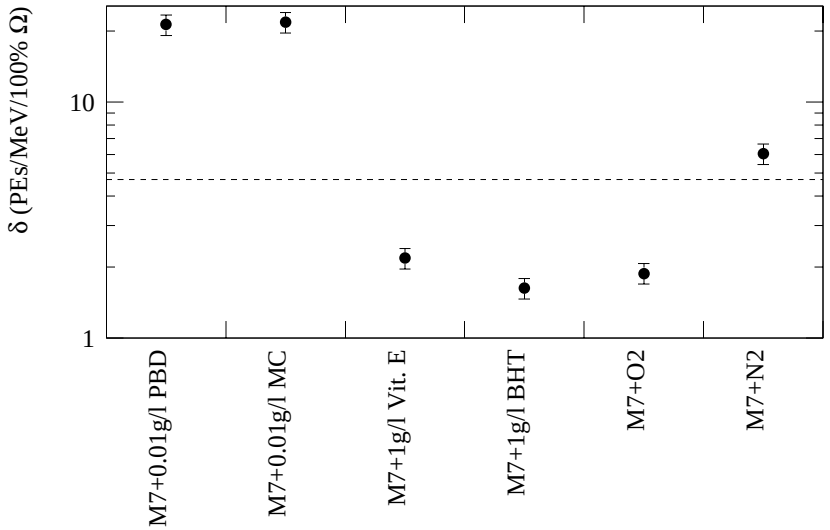

Figure 14: δ values for Marcol 7 with various additives. Note the logarithmic scale. The dotted line indicates the average δ value of $4.7 \pm 0.1 \pm 0.7$ photoelectrons/MeV corrected to 100% solid angle obtained from pure M7 for comparison. The error bars are due to the systematic error on the photoelectron fit. The systematic error from the uncertainty in the effective solid angle of the PMT and the uncertainty in the absolute energy loss of the proton in the oil sample would cause an error in the δ scale of 15%.

Run #	Sample	δ (PE/MeV)
134	M7 + 0.01 g/l PBD	21.25
136	M7 + 0.01 g/l MC	21.79
137	M7 + 1 g/l Vitamin E	2.18
138	M7 + 1 g/l BHT	1.63
150	M7, O2 saturated	1.88
151	M7, N2 saturated	6.05
relative error		$\pm$10%

Table 5: Measured δ values for Marcol 7 (M7) samples with various additives from a set of runs performed in 01/02. The relative error on these measurements is 10% due to uncertainties in the PE fits, the systematic is correlated between measurements and is estimated to be 15%.

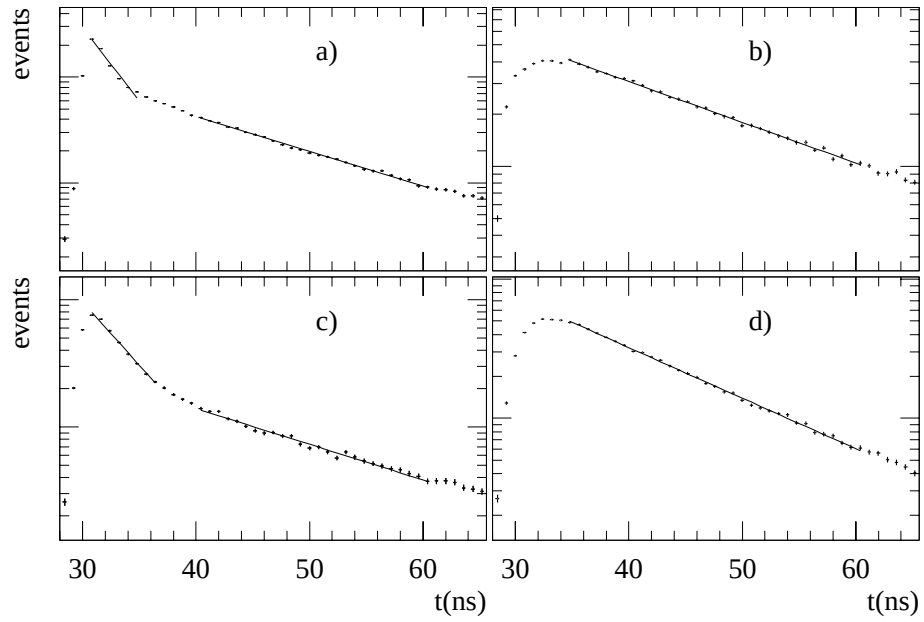

Figure 15: Time distribution fits for oil samples: a) pure Isopar L, b) pure Marcol 7, c) Marcol 7 + 0.01 g/l PBD, d) Marcol 7 + 0.01 g/l MC. Note the logarithmic scale.

from pure Isopar L and pure M7. As can be see in these plots, some distributions are fit better with two exponentials. These results are summarized for all four oils in Table 6.

4.4 Marcol 7 with Gas

The effects of the addition of oxygen and nitrogen can be seen in Table 5 and Figure 14. As mentioned above, the addition of oxygen decreases the light output of the Marcol 7 oil while nitrogen has a smaller effect on the light output, perhaps increasing it slightly. These effects were seen from runs in 01/02 and investigated again in the 07/02 runs using the same samples of oil. The previously bubbled samples of oil (tested 01/02) were left stagnant (in equilibrium with air) for 6 months and were tested again without bubbling. The δ values from these samples returned to (within errors) the original δ values of pure Marcol 7. The samples were then rebubbled to saturate them *again* with nitrogen or oxygen and the δ values had the same behavior as what had been seen in the January 2002 runs. This effect of bubbling, leaving stagnant, and rebubbling, can be seen in Figure 16.

A sample saturated with oxygen reduces the scintillation output by about a factor of 3 as compared to a sample in equilibrium with air. There is slight evidence that a sample saturated with nitrogen has increased

Run #	Sample	τ_f (ns)	τ_s (ns)
multiple	M7, pure, average	-	18.6 ± 1.0
127	Isopar L, pure	3.2	13.2
147	M7 + 0.01 g/l PBD	4.4	15.5
148	M7 + 0.01 g/l MC	-	12.0

Table 6: Time distribution fit results for various oil samples. Some of the distributions were better fit with a "fast" component (τ_f) in addition to the "slow" component (τ_s). The error on τ is explained above for pure M7. For the other sample, the error on the τ values is estimated to be 10%.

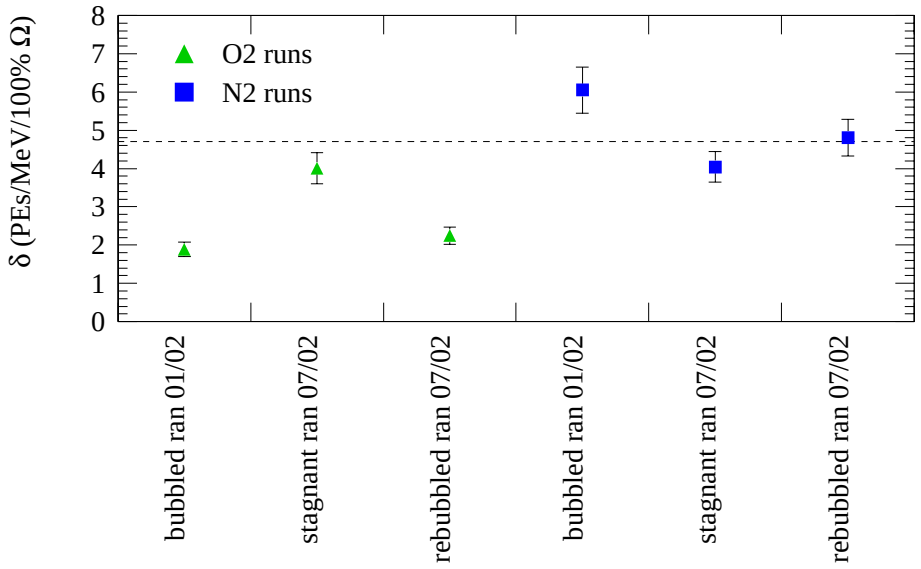

Figure 16: Measured δ values for Marcol 7 bubbled with oxygen and nitrogen. The horizontal line is the average δ value for pure Marcol 7 in equilibrium with air for comparison. Three different runs were done for each type of gas. The Marcol 7 was bubbled with each gas and tested in January 2002. Each of these bubbled samples were left stagnant for 6 months and then tested in 07/02. These samples were then rebubbled and tested again in 07/02.

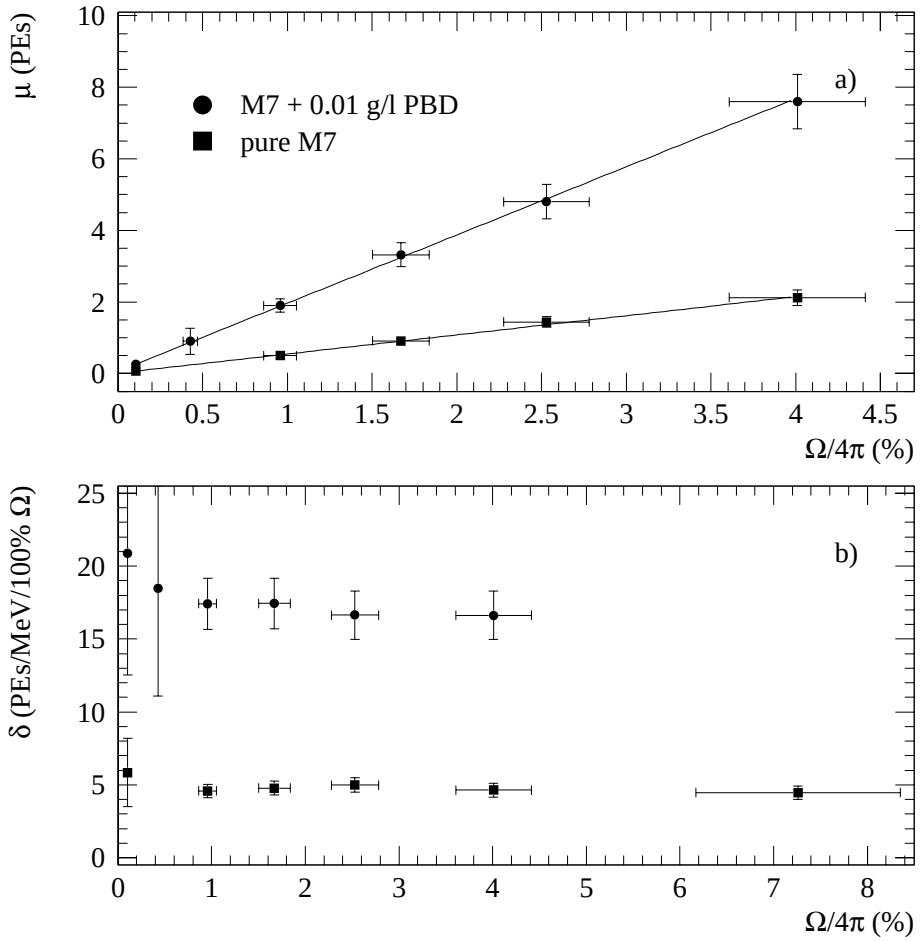

Figure 17: Plots of μ (a) and δ (b) obtained from the solid angle tests for pure M7 and M7 with 0.01 g/l PBD. The point at a solid angle of about 7% is from a test without the mask system, which had a different proton energy loss and could not be plotted in (a). The μ values were well-fit to a linear function (solid lines) constrained to pass through zero.

light by about 20%. Effects this small are difficult to measure conclusively as they are difficult to disentangle with the slight decrease in light output observed from the runs in 01/02 to those in 07/02 as was described in Section 4.1.

4.5 Solid angle tests

As described in Section 2.3, a mask system was constructed and implemented for the 2002 tests. Runs using this system allowed for checks of the robustness of measured δ values by changing the parameters in a well defined way. A total of 7 different solid angles were tested: one for each plug, one of the mask system with no plugs, and one of the PMT solid angle (no mask system). Samples of both pure M7 and M7 with 0.01 g/l PBD were tested with this system.

The results from these variable solid angle runs are shown in Figure 17. Both the μ and δ values are plotted as a function of calculated solid angle for each mask configuration. This data shows that within errors the data behaves as expected. The μ value, which is proportional to the amount of light observed by the PMT, changes linearly with PMT solid angle. The δ value, which is corrected for solid angle and proton track length (via energy loss), remains constant with solid angle. This data provides a check of the calculations of effective solid angle and proton energy loss.

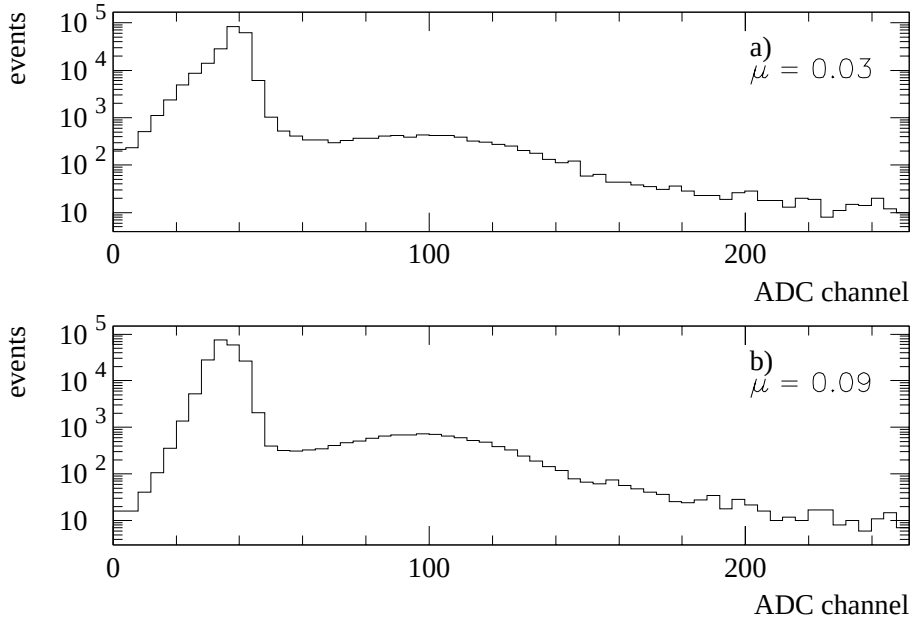

Figure 18: ADC distributions for a) an empty sample beaker and b) a sample of deionized water. Note the logarithmic scale. The average number of photoelectrons as determined by a fit to these spectra are indicated.

4.6 Calibration Runs

To further understand the method and apparatus, an empty sample container (full of "air") and a sample of deionized water were tested. The ADC spectra for these runs are shown in Figure 18. As can be seen in this figure, there is very little light produced in these samples. The amount of light observed in the water is consistent with that predicted by the simulation program (0.1 PE) from the Čerenkov mechanism.

Two calibrators were also constructed during the last set of runs from solid scintillator. The scintillator was covered with black tape except for a small hole which passed light . One calibrator was fabricated with a 1mm hole for low light level calibration, and the other was fabricated with a 5mm hole for high light level calibration. These will be used to monitor changes in the apparatus in future runs.

4.7 Other Oils

Other samples of mineral oil were tested in the 2002 runs. The δ values measured for pure samples of Isopar L and Witco are plotted in Figures 19 and 20. The average δ values obtained are $0.32 \pm 0.01 \pm 0.05$ for Isopar L and $3.9 \pm 0.2 \pm 0.6$ for Witco. The first error is the systematic error in the μ fit (assumed uncorrelated). The second error is due to the uncertainty in solid angle and energy loss.

The same decrease in δ for later runs as was observed for Marcol 7 is seen in these oils. This indicates that it is a real effect. However, it is not outside the errors quoted and investigation into this trend will continue in further tests.

4.8 Optical filters

Two types of optical filters (neutral density and bandpass) were used with the sample mask system. The neutral density filters (25mm Tech Spec^{TM} Absorptive Neutral Density Filters, NT55-222 [4]) transmit a fraction of incident incident that is constant for a large wavelength band. Tests with these filters were performed to better understand the systematic errors of the apparatus. The band pass filters (25mm Commercial Quality Bandpass Filters, NT55-744 [4]) transmit light in certain wavelength bands. These were used in investigate the wavelength dependence of the emitted scintillation light.

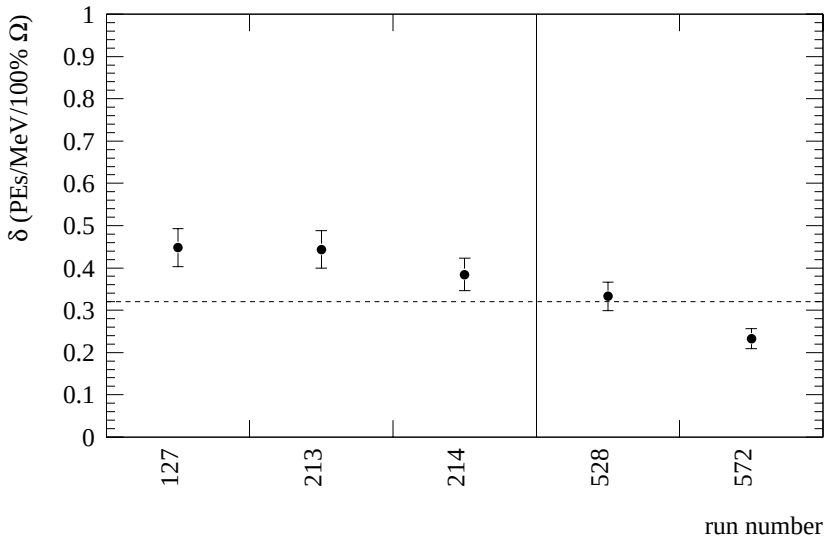

Figure 19: Measured δ values for Isopar L mineral oil. The horizontal line indicates the average value, the vertical line indicates different run periods.

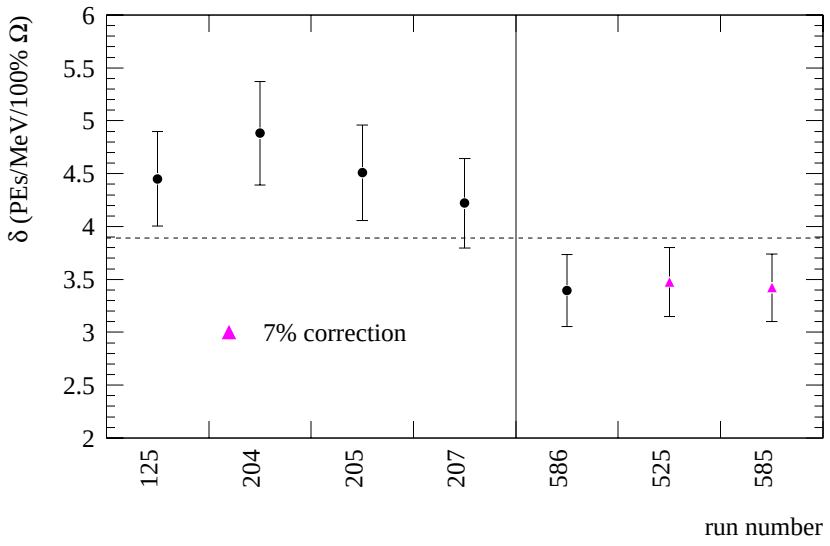

Figure 20: Measured δ values for Witco mineral oil. The horizontal line indicates the average value, the vertical line indicates different run periods.

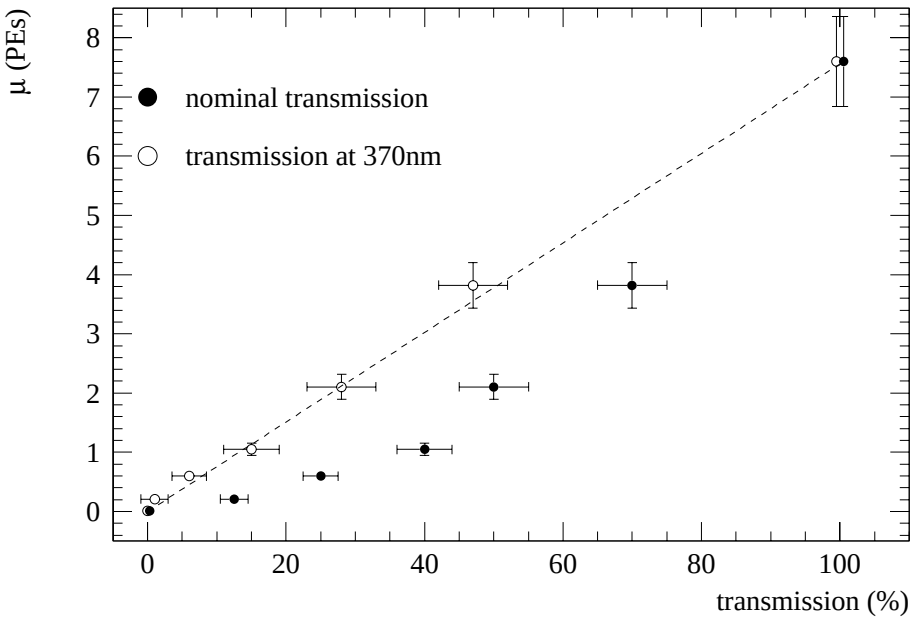

Figure 21: Plots of μ obtained from the neutral density filter tests with M7+0.01 g/l PBD. The closed (open) points are at the nominal (corrected) transmission values. The point at 100% transmission was taken with no filter. The dotted line is a linear extrapolation from the origin to the point at 100% transmission.

4.8.1 Neutral Density filters

The measured μ values are plotted for M7+0.01 g/l PBD in Figure 21. Unfortunately the amount of light emitted from pure M7 was too low to allow tests with the neutral density filters. It was expected that μ extracted from this data would be a linear function with transmission, analogous to that in Figure 17. As can be seen in Figure 21, the amount of light falls off faster with lower transmission than would be expected from the nominal transmission as quoted for the filters. However, upon further examination of the filter specifications, it was noticed that the quoted transmission values are correct only from 450 to 750nm. The filter transmission falls off at the lower wavelengths.

With the hypothesis that the wavelength of emitted light is in a narrow band at 370nm, a corrected transmission value for the filters was obtained. The data is plotted as a function of these corrected transmission values in Figure 21 along with the nominal transmission values. As can be seen in the figure, the neutral density filter data can be explained if the light is emitted from the M7+0.01 g/l PBD sample at around 370nm.

4.8.2 Bandpass filters

The measured δ values for runs with the bandpass filters with pure M7 and for M7+0.01 g/l PBD are summarized in Table 7 together with the filter transmission data. The measured data is difficult to interpret. Data from some of the filters that should pass a subset of wavelengths from another filter, actually seem to pass more light (e.g. compare filters VG6 and BG18). Further tests with this filters are needed to understand this data.

4.9 PMT Comparisons

In order to investigate the dependence of these results on the specific PMT used, an additional Burle 8850 51mm diameter PMT was obtained. This tube has exactly the same specifications as the original and was employed using the same base. Three comparison runs were performed using the two solid scintillator calibrators and the pure M7 sample. These three runs should be identical in all other ways. Figure 22 shows

filter name	central λ (nm)	FWHM λ (nm)	pure M7 δ (PE/MeV)	M7+ 0.01g/l PBD δ (PE/MeV)
BG38	470	271	0.57	13.87
BG18	493	160	0.09	3.24
BG12	407	104	0.13	7.66
VG6	520	92	0.02	6.19
VG9	526	53	3.02	not tested
RT830	830	260	0.04	0.02
U330	330	140	4.05	11.57
U340	340	85	0.02	0.02
no filter	–	–	4.71	17.4

Table 7: Measured δ values for different bandpass filters with pure M7 and M7+0.01g/l PBD. The relative error is 10% for δ values above 0.1 and 100% below.

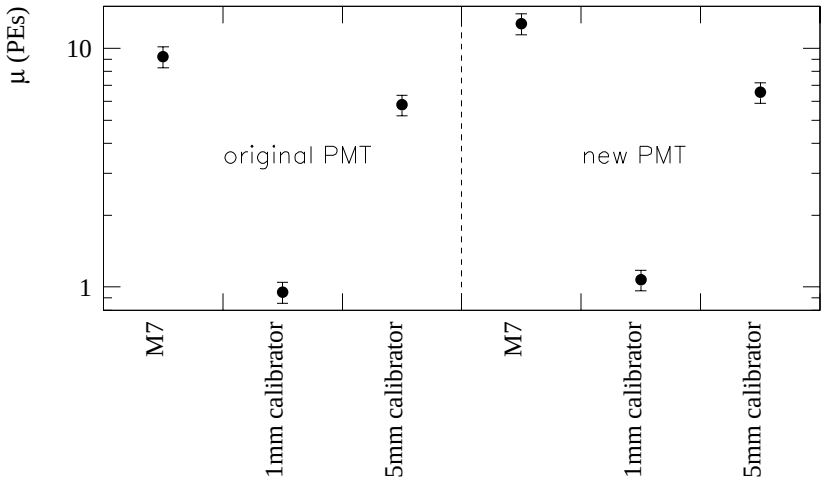

Figure 22: Measured μ values from pure Marcol 7 and the two solid scintillator calibrators for the original PMT compared to the new PMT.

the measured μ values obtained in these runs with the new tube together with the analogous runs with the original PMT. With the exception of a slight difference in the μ value for the pure M7 runs, the values agree well.

To investigate this further, tests were also performed to compare the original PMT to the new. In these tests a pulsed LED with a stack of differing numbers of identical filters was used to produce light at known levels. The original PMT was tested using these filters and compared with the new PMT. The results of this study are plotted in Figure 23. This plot shows reasonable agreement between the two PMTs.

4.10 Comparison of 2001 and 2002 Data

The tests performed in 2002 included samples tested in 2001 to check the long term reproducibility of these methods as well as any chemical changes in the samples that may have occurred in the 10 months between. A comparison of results from samples that were retested showed a surprising and not completely understood effect.

A change in light output was first noticed for a sample of pure Witco mineral oil. This sample was tested in various experimental configurations in 2001 and then retested in 2002. This sample had been sitting in

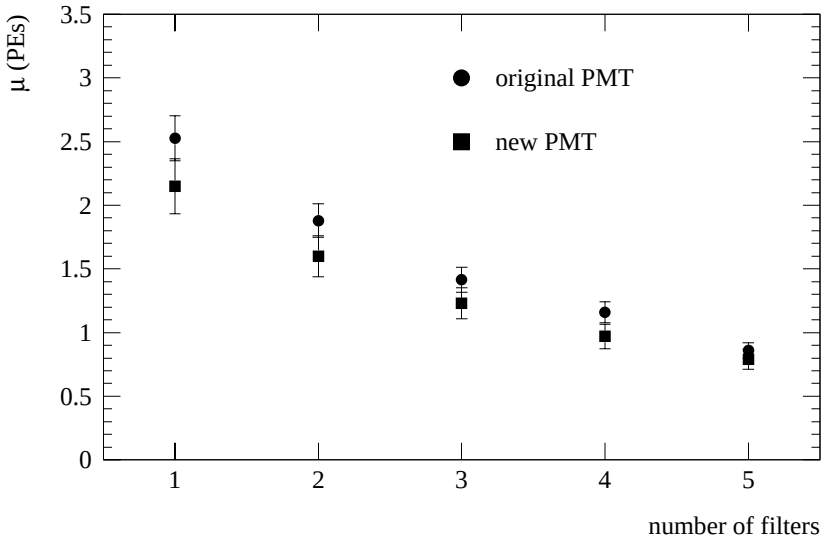

Figure 23: Measured μ values for the original and new PMTs in tests with an LED light source and different numbers of identical filters.

the sample beaker for 10 months (exposed to the anodized Al in the sample container). Also, a fresh sample of Witco from the the original volume was poured into a clean sample beaker. The results of these runs are shown in Figure 24. They show that the sample tested in 2001 produced approximately a factor of two less light than the samples tested in 2002, including the sample freshly poured,

The pure Isopar L sample tested in 2001 exhibited a similar behavior as did the pure Witco. A comparison of pure Isopar L samples, including a freshly poured sample is shown in Figure 25. For several of these tests the voltage on the tube was changed in order to understand any effect of differing PMT voltage settings. The different PMT voltage value has no effect, as is expected with the analysis method used.

The same trend can be seen in Figure 26 which shows samples of Witco with 0.01 g/l of PBD. Again, a sample freshly poured and mixed in 2002 was tested.

Figure 27 shows a comparison of the ADC spectra for the same pure Witco sample tested in 2001 and 2002. The μ values are indicated. As the gain of the PMT is determined in the photoelectron fit procedure, it is not likely that a change in gain of the PMT can explain the differences seen in the light output.

The reason for the change in light output from the 2001 to 2002 tests on these three samples of oil has been determined. The PMT base was modified slightly in between the 2001 and 2002 runs. This was a change to the voltage divider circuit for the second dynode of the PMT. It was initially thought that the change should have a negligible effect on the PE collection efficiency. However, further tests using a pulsed light source in the lab to compare the two base configurations showed that the first base configuration was not optimal and resulted in an lower gain and a lower *effective* quantum efficiency. For the 2002 tests, the base configuration was close to optimal no correction to the PMT quantum efficiency is needed. The details of the base tests are included in an Appendix to this document.

4.11 Results from 2001 Data

It has been determined that the results from the 2001 data include an reduction in the effective quantum efficiency of the PMT by about 50%. No attempt is made to include that effect, however, it is assumed that results from 2001 that involve *relative* comparisons of data are valid. These results are reported in the following sections.

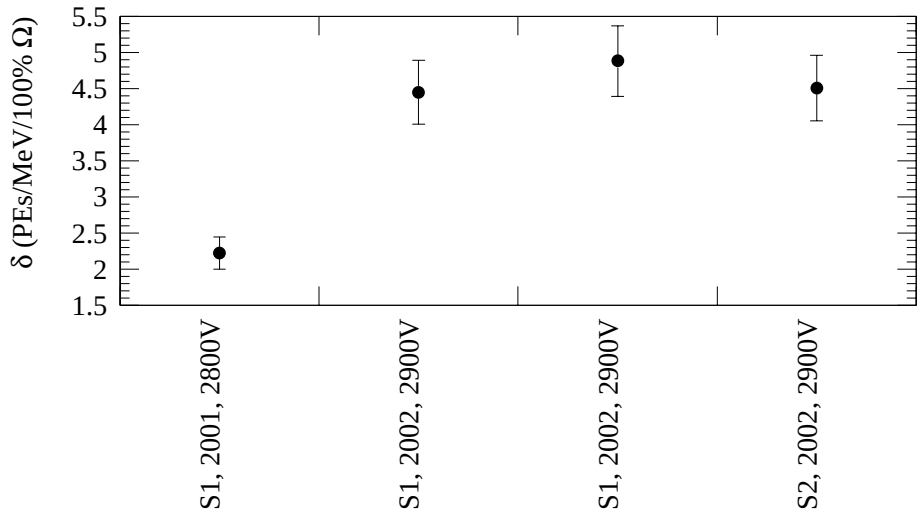

Figure 24: Comparison of δ values for pure Witco samples. Compared are 2 different samples (S1,S2) in 2001 and 2002 runs at different PMT voltages. Sample #1 (S1) was the same oil in the same sample container as was tested in 2001. Sample #2 (S2) was freshly poured in 2002.

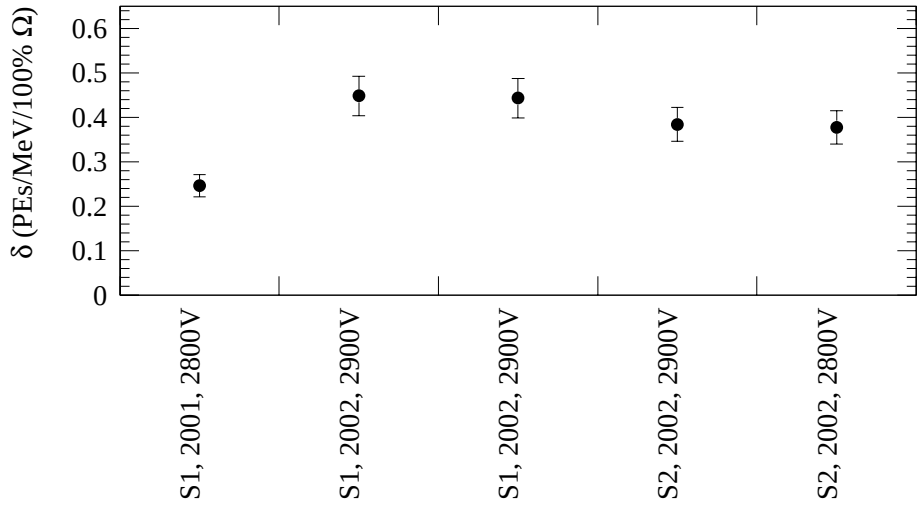

Figure 25: Comparison of δ values for Isopar L samples. Compared are 2 different samples (S1,S2) in 2001 and 2002 runs at different PMT voltages. Sample #1 (S1) was the same oil in the same sample container as was tested in 2001. Sample #2 (S2) was freshly poured in 2002.

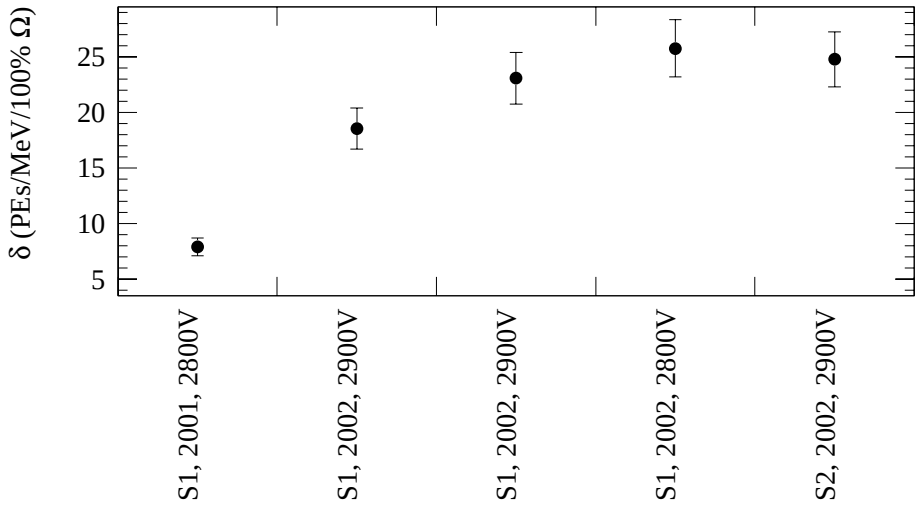

Figure 26: Comparison of δ values for Witco + 0.01 g/l PBD samples. Compared are 2 different samples (S1,S2) in 2001 and 2002 runs at different PMT voltages. Sample #1 (S1) was the same oil in the same sample container as was tested in 2001. Sample #2 (S2) was freshly mixed and poured in 2002.

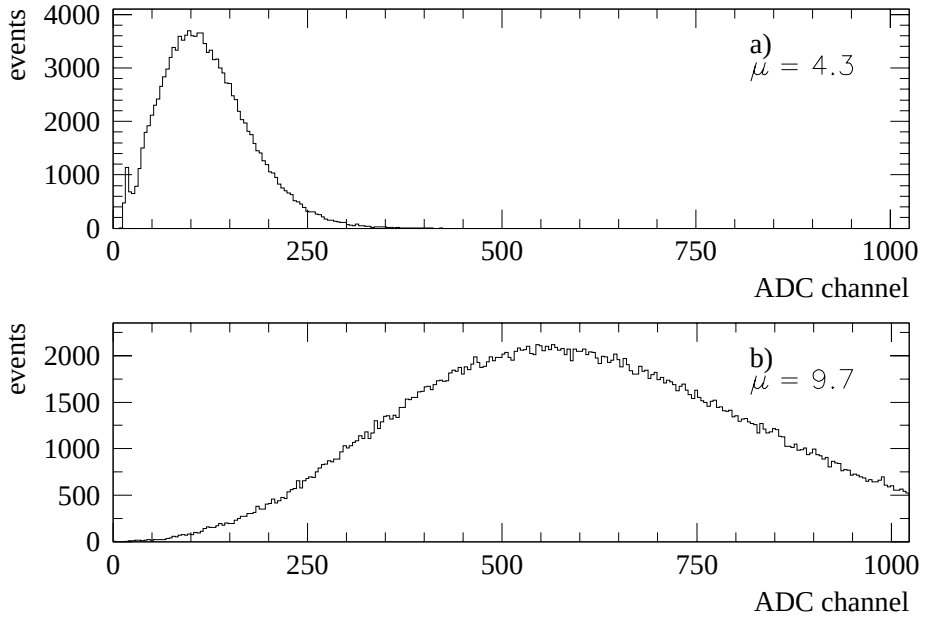

Figure 27: ADC spectra from a run with the same pure Witco sample in a) 03/01 and b) 03/02. The average number of photoelectrons as determined by a fit to these spectra are indicated.

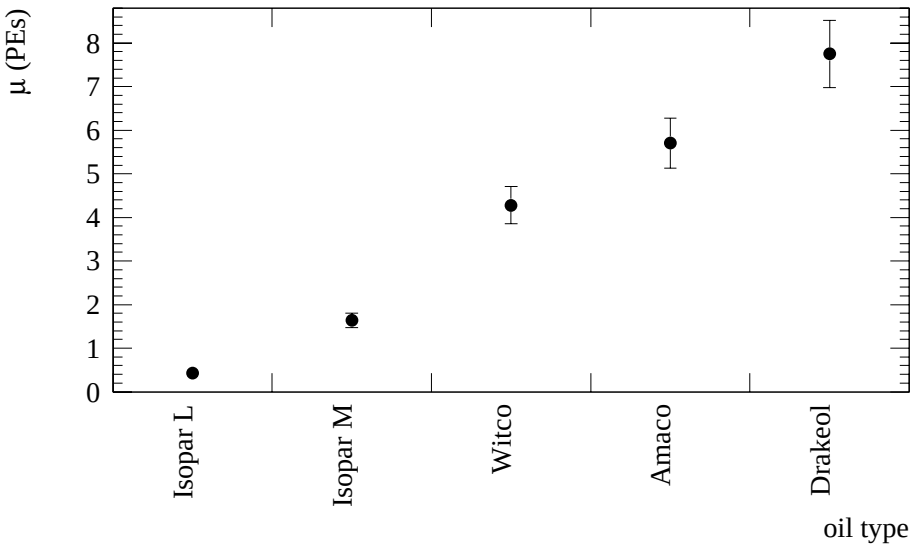

Figure 28: Measured μ for five different pure mineral oils tested in 2001.

4.11.1 Pure Mineral Oils

Five different pure mineral oils with no additives were tested. These were candidate oils for the MiniBooNE detector at the time. The results are summarized in Figure 28.

4.11.2 Mineral Oil with Scintillator

Samples of Witco mineral oil with concentrations of PBD scintillator from 0.01 to 2.0 g/l were also tested. These results are shown in Figure 29.

Samples of both Witco and Isopar L mineral oil containing small quantities of PBD and MC scintillators were tested. These results are shown in Figure 30.

4.11.3 Saturation

To investigate any nonlinear energy dependence of the light output from the mineral oil samples, tests were performed with the degrader system. This system used differing thickness of Copper plates in the beam, upstream of the samples to "degrade" the energy of the beam. Plates of thickness 0.50, 0.75, 1.0, and 1.128 inches were used. Together with the data taken with no degrader, this allowed tests of light output with 5 different proton energy loss values. However, not all plates were used with every sample. Tests were performed with this system on samples of pure Witco, pure Isopar L, and Isopar L with 0.03 g/l of MC. The results are shown in Figure 31.

The GEANT simulation program was used to calculate the proton energy loss in the oil sample. It was also used to calculate the energy loss corrected for saturation using Birk's Law [2],

$$\frac{dE'}{dx} = \frac{\frac{dE}{dx}}{1 + kB(\frac{dE}{dx})},$$

where $\frac{dE'}{dx}$ is the corrected energy loss and $\frac{dE}{dx}$ is the uncorrected. The parameter kB was set to 0.0146 g/cm^2/MeV. This value was measured for anthracene [5] and is similar to that used (0.014 g/cm^2/MeV) in the current version of the MiniBooNE detector Monte Carlo Program. This correction was applied for each proton tracking step and then totaled for each proton track through the sample. The corrected energy loss obtained is lower than the uncorrected as can be seen in Figure 31 (each closed point has a corresponding open point at a lower energy).

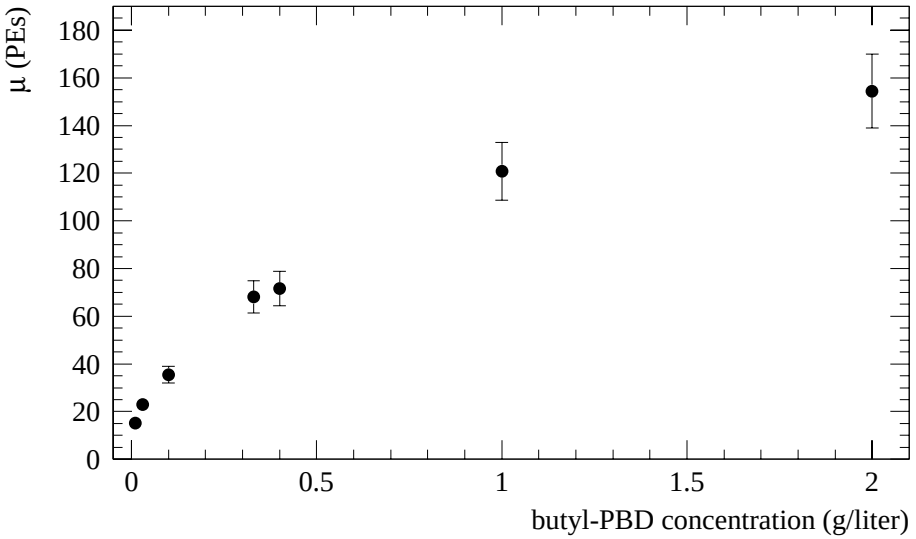

Figure 29: Measured μ values for different concentrations of PBD scintillator in Witco mineral oil.

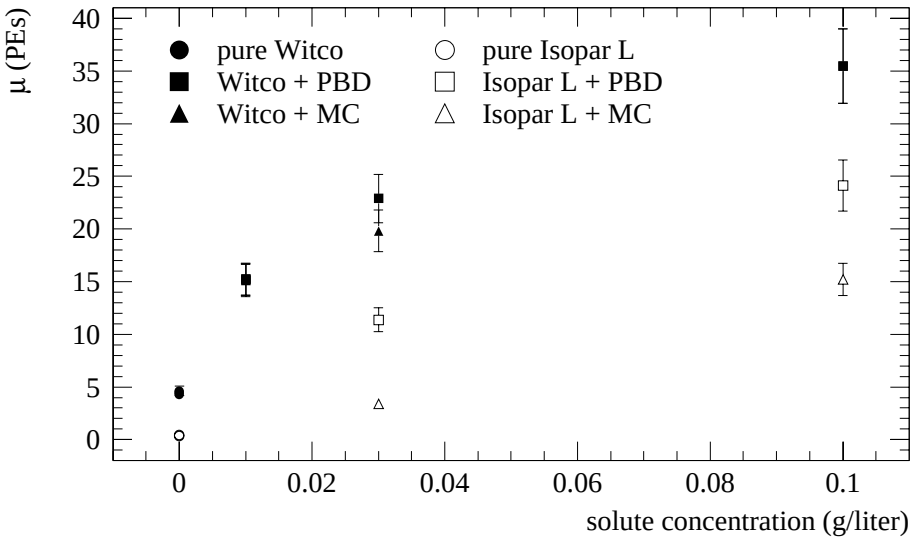

Figure 30: Measured μ values for different concentrations of PBD and MC in Witco and Isopar L mineral oils.

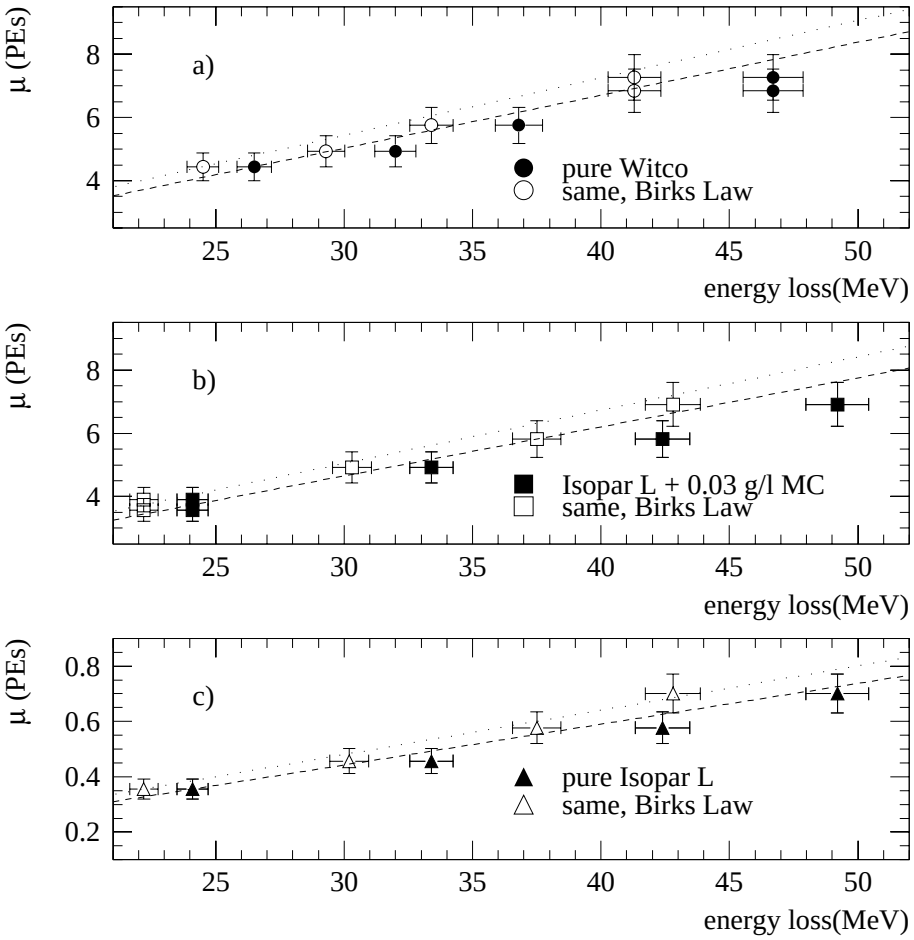

Figure 31: Measured μ values from saturation tests in samples of pure Witco (a), Isopar L with 0.03 g/l of MC (b), and pure Isopar L (c) as a function of proton energy loss with (open points) and without (closed points) a Birk's Law correction. The dotted (dashed) lines show a linear extrapolation from the origin through the first corrected (uncorrected) data point.

The uncorrected data lies slightly below a linear extrapolation from zero for all three samples tested. The corrected data lies closer to the linear extrapolation, however, given the errors on these measurements, the data is not inconsistent with either model. More work is needed to make a conclusive measurement of saturation.

5 Conclusions

An experimental method to test the scintillation properties of mineral oil has been developed and implemented at the Indiana University Cyclotron Facility. The measured scintillation light output of the MiniBooNE detector mineral oil, Marcol 7, from 180 MeV protons is $4.7 \pm 0.1 \pm 0.7$ PEs/MeV corrected to 100% detected solid angle. The time distribution of this light is well-fit to a single exponential distribution with a characteristic time of 18.6 ± 1.0 ns. In addition, other tests were performed on a variety of oil samples with different additives.

These results have been demonstrated to be robust in a variety of ways. The incompatibility between 2001 and 2002 tests is now understood and it is believed that the absolute light output as measured in the 2002 tests is correct to within the errors quoted. Several interesting effects observed in tests using neutral density and bandpass optical filters have been identified and will be pursued in future work.

References

[1] http://www.burle.com/cgi-bin/byteserver.pl/pdf/8850.pdf

[2] J. B. Birks, *The Theory and Practice of Scintillation Counting*, (Macmillan, New York, 1964).

[3] *GEANT Detector Description and Simulation Tool*, (CERN, Geneva, Switzerland, 1993).

[4] Edmund Optics, http://www.edmundoptics.com

[5] R. L. Craun and D. L. Smith, Nucl. Instr. and Meth **80**, 239 (1970).

6 Appendix: PMT Base Configuration Tests

Tests were performed on the base used for Burle 8850 PMT. These tests show that the factor of 2 discrepancy in the 2001 data to be caused by a resistor change in the base. An optimal setting of the potentiometer was also determined.

6.1 Introduction

Oil tests were performed at the IUCF in March 2001, and January, March, and July 2002. In these these tests, the average number of PEs seen in each sample of oil as protons travel through it (μ value) was extracted. This μ value was normalized to 100% solid angle and per 1 MeV (δ value). The results from 2001 seem to be consistent relative to each sample but they differ by a factor of 2 when compared to the results of the runs in 2002.

After the tests in 2001, only a few parameters changed in our setup. One of these parameters was the configuration of the PMT base. In accordance with the manufacturer, the voltage difference between dynodes 1 and 2 was changed to 4%. This was done by changing the resistor R13 from 68kΩ to 100kΩ (see Figure 32). This effectively changed the voltage drop between dynodes 1 and 3 with respect to the total voltage drop. The potentiometer R15 was also changed to control the voltage drop between dynodes 1 and 2 and dynodes 2 and 3 (see Table 8).

6.2 Tests

The effect of this base configuration change was tested by using another base (base 3) with the PMT used in the oil tests. A pulser and an LED were used to produce light. The light was attenuated so it produced a spectrum where the first and second PE peaks could be seen. This meant a μ value of 1.4 with the standard base (base 0).

Base 3 was tested with this setup. The configuration of base 3 was such that the resistor R13 was 68kΩ. This was the configuration that was used in the 2001 runs (see Table 8). With base 3 in the 2001 configuration, an average of 0.79 ± 0.03 PEs were seen. Base 3 was then removed and the resistor R13 was replaced with a 100kΩ resistor. The POT R15 was then changed so the configuration was the same as the current standard configuration with base 0. This produced a μ value of 1.47 ± 0.06 PEs seen. Base 0 was also tested before and after base 3 to ensure that the light output of the LED did not change and that the modified configuration of base 3 produced the same μ value as the standard base 0.

These μ values were obtained by fitting a function to the spectra produced. The μ values taken from these fits can be seen in Figure 33. From this plot, a factor of 2 change in the μ value can be seen at the two different configurations of base 3. The modified configuration of base 3 matches the standard configuration that we use for base 0 so the μ values agree. The fits can be seen in Figures 35 and 36. Another method of finding the μ values was also used which counted the number of zeroes in the pedestal. The μ values obtained from this method were in agreement with the μ values from the fits.

The gain also changes in the two spectra. This is an effect that is also a result of the voltage drop change between the dynodes. The gain changes caused by the base modifications can be seen in Figure 34. The gain and μ are lower for the base 3 2001 configuration. A lower gain does not necessarily imply a lower μ value. In fact, for a properly configured base, the gain is independent of the μ value as is shown in the next subsection.

6.3 Optimal Settings

Separate tests were done to determine the optimal settings of the base for future runs. In these tests, a base was used (base 1) in the modified configuration (see Table 9). The POT R15 was used to control the voltage drop apportionment to dynodes 1 and 2 and dynodes 2 and 3. The voltage drop from dynodes 1 to 3 was fixed at 10%. The POT was turned all the way counter clockwise so the voltage drop between dynodes 1 and 2 was 3%. (This forced the voltage drop between dynodes 2 and 3 to be 7%.) The voltage drop between dynodes 1 and 2 was then increased in 1% increments until the POT was all the way clockwise. Fits were done on these spectra and the μ values and gains were plotted verses the voltage drop (see Figures 37 and 38).

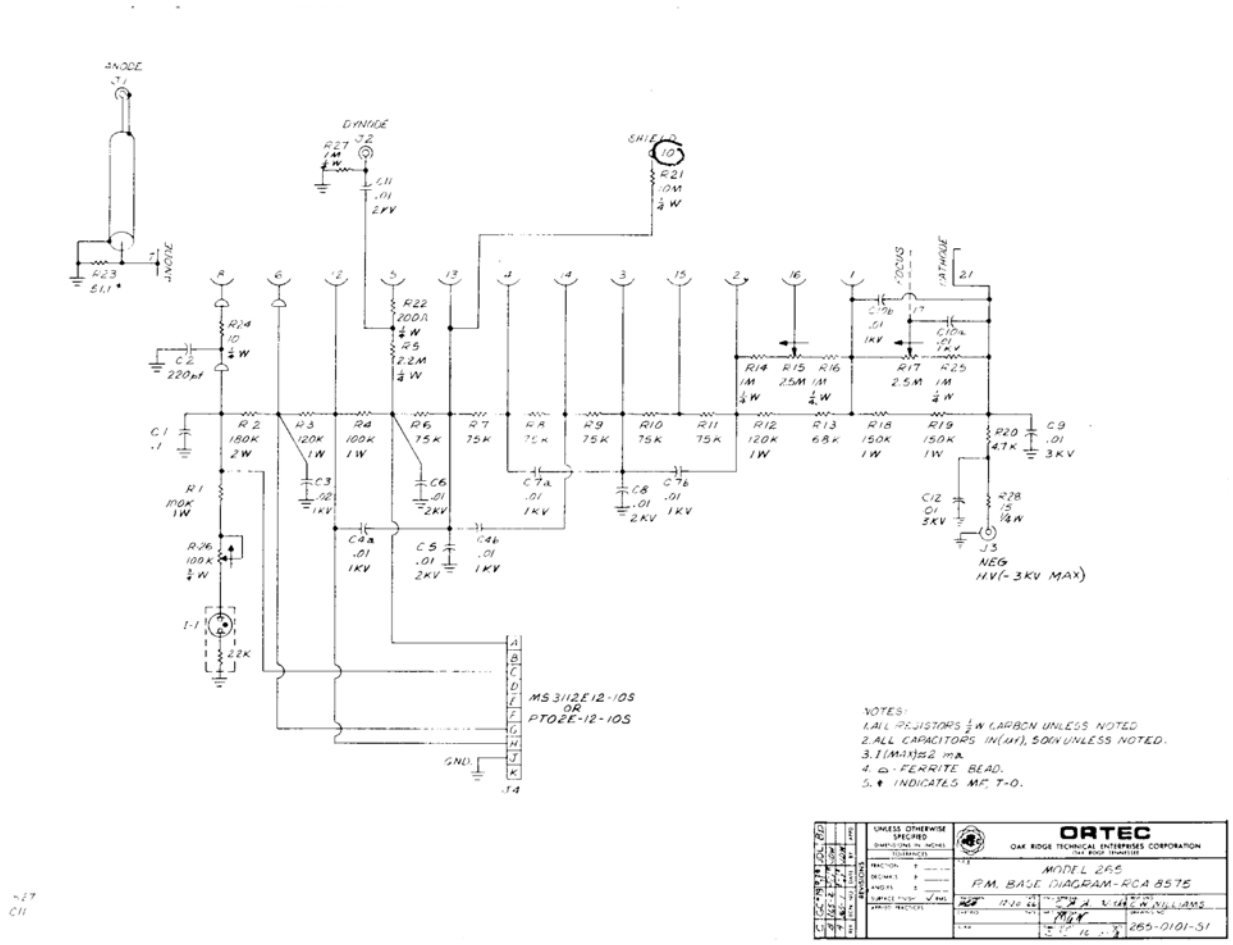

Figure 32: Schematic for the 256 base as we received it. R19 was replaced with a 470kΩ resistor before any use in 2001. Later (after 2001 runs) R13 was changed to 100kΩ and the POT R15 was tuned to improve PE peak resolution.

Dynode #	Pin #	% voltage drop 2001 configuration	% voltage drop modified configuration
Cathode	21		
		30.0	29.5
1	1		
		1.9	3.9
2	16		
		7.2	6.2
3	2		
		4.2	4.1
4	15		
		4.1	3.9
5	3		
		4.1	4.0
6	14		
		4.1	4.0
7	4		
		4.1	3.2
8	13		
		3.3	3.2
9	5		
		4.5	4.4
10	12		
		6.6	6.4
11	6		
		10.1	9.9
12	8		
		10.9	10.7
Anode	7		

Table 8: The % voltage drops between each pair of dynodes for the 2001 and modified configurations. These dynodes as well as the anode and cathode correspond to a pin # that can be found on the schematic. Note that the main changes occur between dynodes 1 and 2 and dynodes 2 and 3. This is because the resistor that was changed R13 was in parallel with these dynodes (see Figure 32).

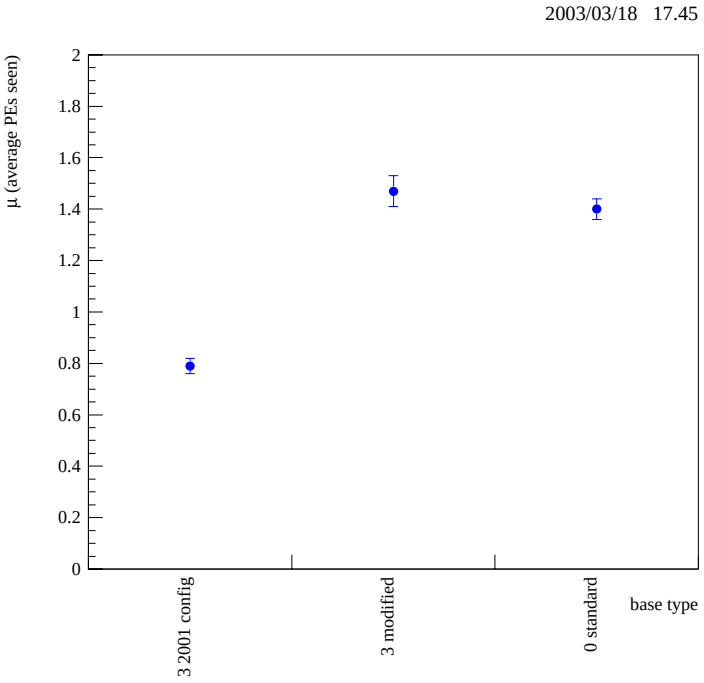

Figure 33: μ values at from different configurations of base 3 and from the standard base 0. The errors shown come from a $\pm 6\%$ error on the fit and on any changes in the light output of the LED.

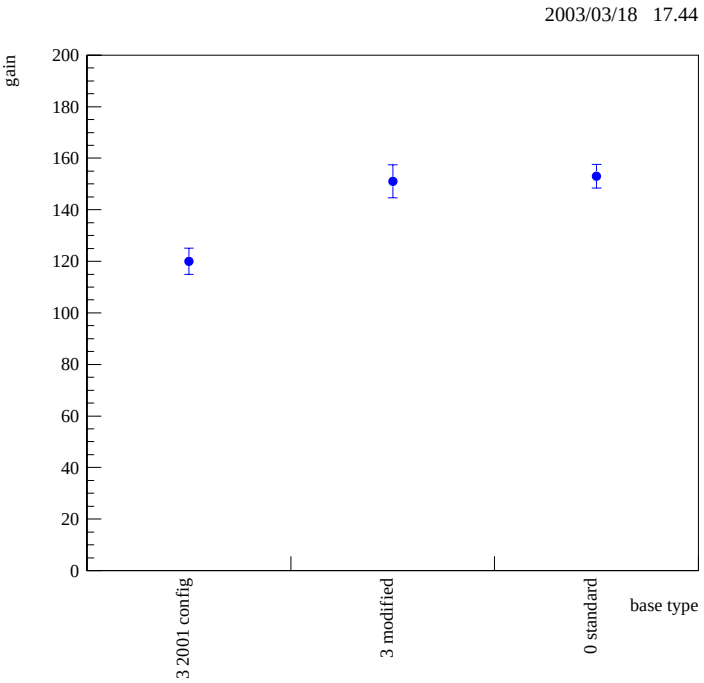

Figure 34: The gains from different configurations of base 3 and from the standard base 0. The errors shown come from a $\pm 6\%$ error on the fit.

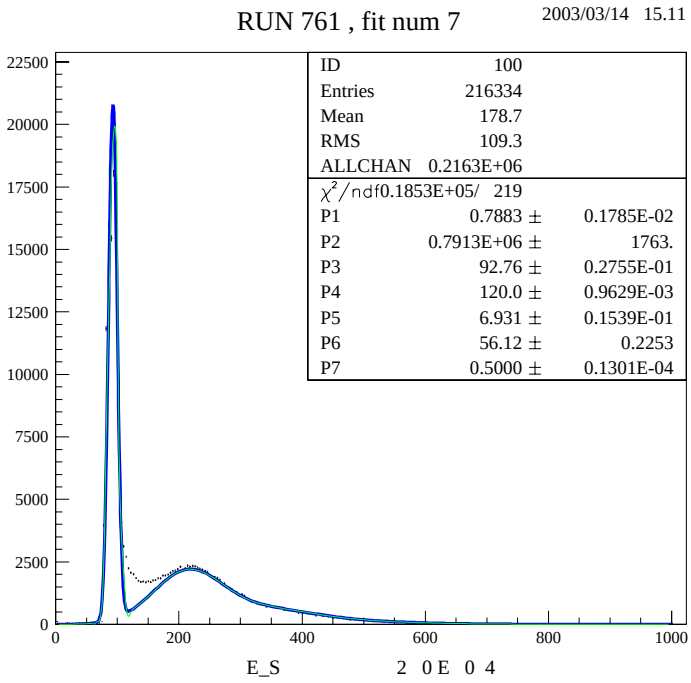

Figure 35: ADC spectrum for base 3 using the 2001 configuration. Note that the pedestal is larger in comparison to the PE peaks than in Figure 36. The solid line is the fit done on the spectrum which produced a μ of 0.79 PEs seen.

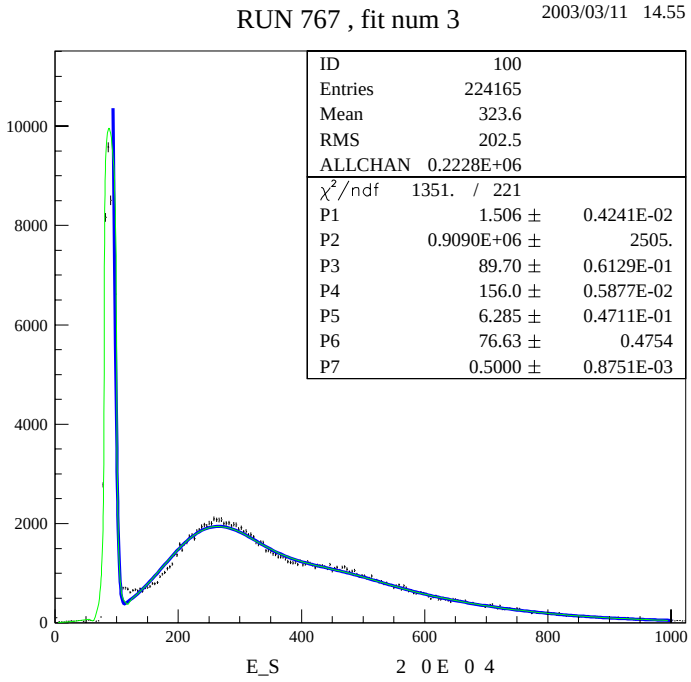

Figure 36: ADC spectrum for base 3 using the 2002 configuration. Note that there is more light than in Figure 35. The solid line is the fit done on the spectrum which produced a μ of 1.51 PEs seen.

Dynode #	Pin #	% voltage drop optimal configuration
Cathode	21	
		29.1
1	1	
		5.0
2	16	
		5.2
3	2	
		4.1
4	15	
		4.1
5	3	
		4.0
6	14	
		4.0
7	4	
		4.0
8	13	
		3.2
9	5	
		4.3
10	12	
		6.4
11	6	
		10.0
12	8	
		10.7
Anode	7	

Table 9: The% voltage drops between each pair of dynodes for the optimal voltage settings. These dynodes as well as the anode and cathode correspond to a pin # that can be found on the schematic.

Many runs were also done during this time with base 0 to ensure that the light output of the LED remained unchanged and to estimate the error due to removing and installing the base repeatedly (see Figure 39).

The results of these tests showed that the μ value did not change as a function of the voltage drop between dynodes 1 and 2 as long as the voltage drop between dynodes 1 and 3 was the same. The gain, however, did change. The optimal settings for future runs should be such that no light is lost and therefore the μ value is the highest, and that the gain is maximized. These conditions can be met if the dynode voltage drop between 1 and 2 is 5%. This maximizes gain and does not effect the μ value so a direct comparison can be made with all previous runs after 2001.

6.4 Conclusions

These tests show that the change in the R13 resistor causes a change in the measured amount of light seen by a factor of 2. This must be due to bad focusing in the early stages of the dynode chain which causes some electrons to be "lost". This explains the discrepancy between the 2001 and subsequent runs.

There is also a change in the gain as the dynode 1 and 2 voltages change. This gain can be maximized by running with the configuration laid out in Table 9. Changing the potentiometer to make the voltage drop between dynodes 1 and 2 5% will maximize the gain but does not change the μ value.

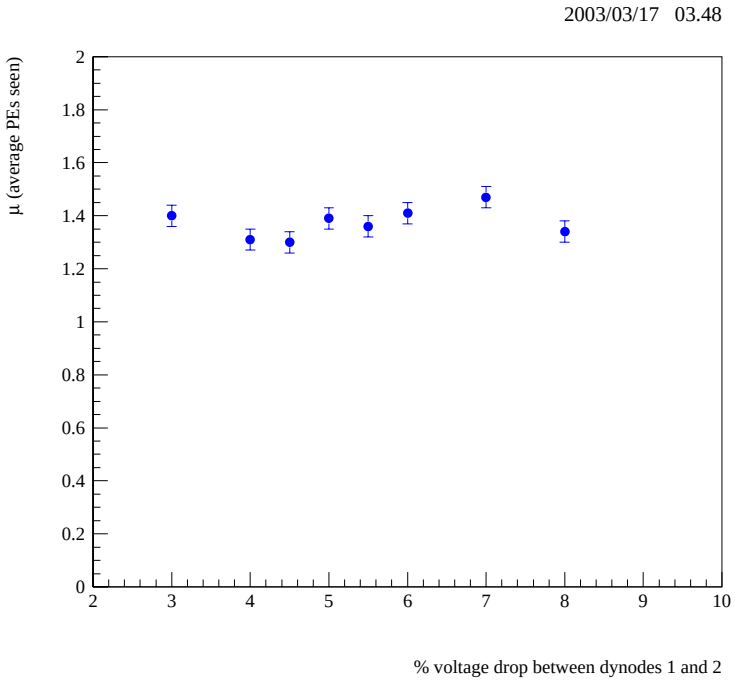

Figure 37: μ verses the % voltage drop between dynodes 1 and 2. Note that the μ value did not change as a function of voltage drop. The errors shown are a $\pm 3\%$ error due to the fits and the change in setup such as light output fluctuation from the LED.

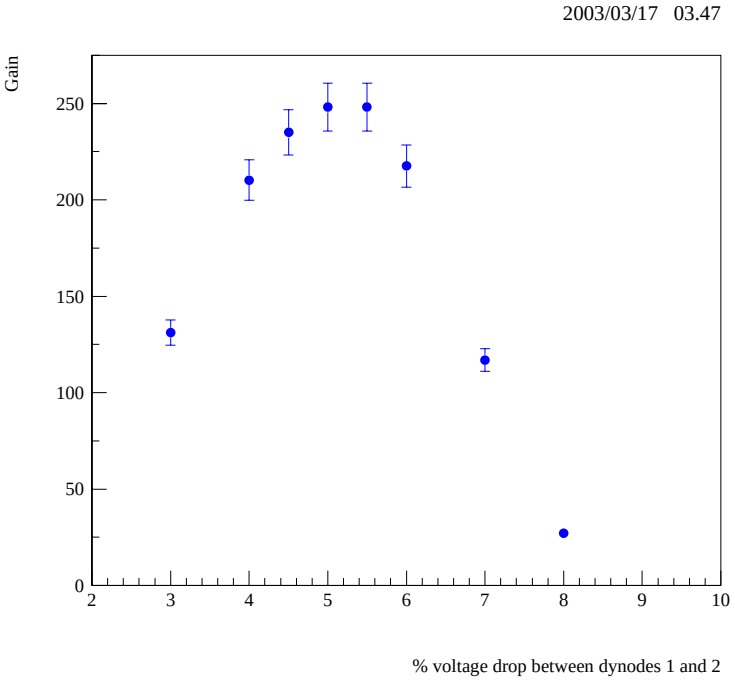

Figure 38: Gain verses the % voltage drop between dynodes 1 and 2. The optimal settings can be seen where the gain is maximized at 5%. The errors shown are a 5% error that come from the fits.

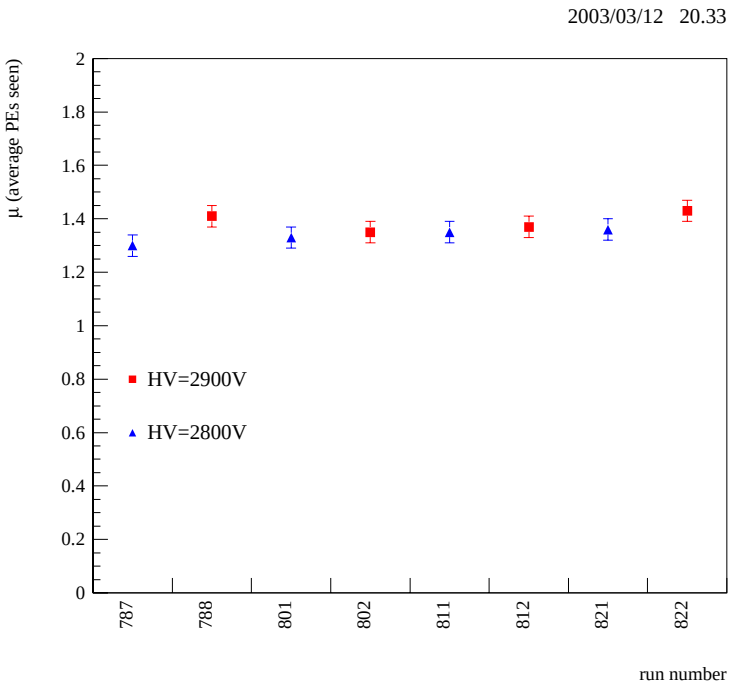

Figure 39: μ for various runs using base 0 in the standard configuration. μ stayed fairly constant which indicates that the LED light output remained the same and that the tube could be replaced in the same position with little error. The errors shown are a $\pm 3\%$ error due to the fits and the change in setup such as light output fluctuation from the LED.